

# Geochemistry, Geophysics, Geosystems

## RESEARCH ARTICLE

10.1029/2018GC007985

### Key Points:

- Within the 645-m Tutuila drill core we find isotopically heterogeneous lavas as well as several abrupt temporal and geochemical boundaries
- The proximity of Samoan volcanoes to the Tonga Trench and geochronology are consistent with a tectonic influence on rejuvenated volcanism
- The tectonic setting and isotopic signatures of the Samoan rejuvenated lavas link them to “petit spots” outboard of the Japan Trench

### Supporting Information:

- Supporting Information S1
- Table S1
- Table S2
- Table S3
- Table S4

### Correspondence to:

A. A. Reinhard,  
reinhard@ucsb.edu

### Citation:

Reinhard, A. A., Jackson, M. G., Blusztajn, J., Koppers, A. A. P., Simms, A. R., & Konter, J. G. (2019). “Petit spot” rejuvenated volcanism superimposed on plume-derived Samoan shield volcanoes: Evidence from a 645-m drill core from Tutuila Island, American Samoa. *Geochemistry, Geophysics, Geosystems*, 20, 1485–1507. <https://doi.org/10.1029/2018GC007985>







Received 25 SEP 2018

Accepted 7 FEB 2019

Accepted article online 13 FEB 2019

Published online 21 MAR 2019

## “Petit Spot” Rejuvenated Volcanism Superimposed on Plume-Derived Samoan Shield Volcanoes: Evidence From a 645-m Drill Core From Tutuila Island, American Samoa

Andrew A. Reinhard<sup>1</sup> , Matthew G. Jackson<sup>1</sup> , Jerzy Blusztajn<sup>2</sup> , Anthony A. P. Koppers<sup>3</sup> , Alexander R. Simms<sup>1</sup> , and Jasper G. Konter<sup>4</sup> 

<sup>1</sup>Department of Earth Science, University of California, Santa Barbara, CA, USA, <sup>2</sup>Woods Hole Oceanographic Institution, Woods Hole, MA, USA, <sup>3</sup>College of Earth, Ocean, and Atmospheric Sciences, Oregon State University, Corvallis, OR, USA, <sup>4</sup>Department of Earth Sciences, University of Hawai‘i at Mānoa, Honolulu, HI, USA

**Abstract** In 2015 a geothermal exploration well was drilled on the island of Tutuila, American Samoa. The sample suite from the drill core provides 645 m of volcanic stratigraphy from a Samoan volcano, spanning 1.45 million years of volcanic history. In the Tutuila drill core, shield lavas with an EM2 (enriched mantle 2) signature are observed at depth, spanning 1.46 to 1.44 Ma. These are overlain by younger (1.35 to 1.17 Ma) shield lavas with a primordial “common” (focus zone) component interlayered with lavas that sample a depleted mantle component. Following ~1.15 Myr of volcanic quiescence, rejuvenated volcanism initiated at 24.3 ka and samples an EM1 (enriched mantle 1) component. The timing of the initiation of rejuvenated volcanism on Tutuila suggests that rejuvenated volcanism may be tectonically driven, as Samoan hotspot volcanoes approach the northern terminus of the Tonga Trench. This is consistent with a model where the timing of rejuvenated volcanism at Tutuila and at other Samoan volcanoes relates to their distance from the Tonga Trench. Notably, the Samoan rejuvenated lavas have EM1 isotopic compositions distinct from shield lavas that are geochemically similar to “petit spot” lavas erupted outboard of the Japan Trench and late stage lavas erupted at Christmas Island located outboard of the Sunda Trench. Therefore, like the Samoan rejuvenated lavas, petit spot volcanism in general appears to be related to tectonic uplift outboard of subduction zones, and existing geochemical data suggest that petit spots share similar EM1 isotopic signatures.

## 1. Introduction

Samoan volcanoes display a wide range of radiogenic isotopic compositions (Hart et al., 2004; Jackson et al., 2010, 2014, 2007; Konter & Jackson, 2012; Workman et al., 2004; Wright & White, 1987); however, the relationship between these isotopic compositions and the stages of volcanism has not been closely examined. Previous work has identified three stages of volcanism in the Samoan hotspot: a shield stage of volcanism, followed by caldera collapse and caldera infilling with differentiated lavas, which is in turn followed by a hiatus in volcanism that ends with rejuvenated volcanism veneering the shield stage (Stearns, 1944; Natland, 1980). Several other studies have noted that the rejuvenated stage of volcanism in Samoa is geochemically distinct from the shield stage (Hart et al., 2004; Konter & Jackson, 2012; Wright & White, 1987; Workman et al., 2004). However, identifying geochemical distinctions within the Samoan shield stage is challenging due to the limited subaerial sampling and the relatively few deep submarine dredges from a small number of volcanoes.

One method of constraining the life cycle of a shield volcano is deep drilling and coring. While drilling provides only a limited, one-dimensional record of volcano evolution, it can yield the most stratigraphically complete record of volcanism at a given location. Previous work has utilized drilling to constrain hotspot volcano evolution at, for example, Hawai‘i (e.g., Garcia et al., 2007; Kurz et al., 1996; Lassiter et al., 1996), Louisville (Koppers & Sager, 2014), Marquesas (Caroff et al., 1999), Kerguelen (Neal et al., 2002; Wallace et al., 2002; Weis & Frey, 2002), and Iceland (e.g., Flower et al., 1982). However, to date there has been no Samoan drilling project.

In 2015, a 645-m geothermal exploration well was drilled on the Samoan Island of Tutuila for the American Samoa Power Authority. The core samples from this drill hole provide the basis for this study. Here we

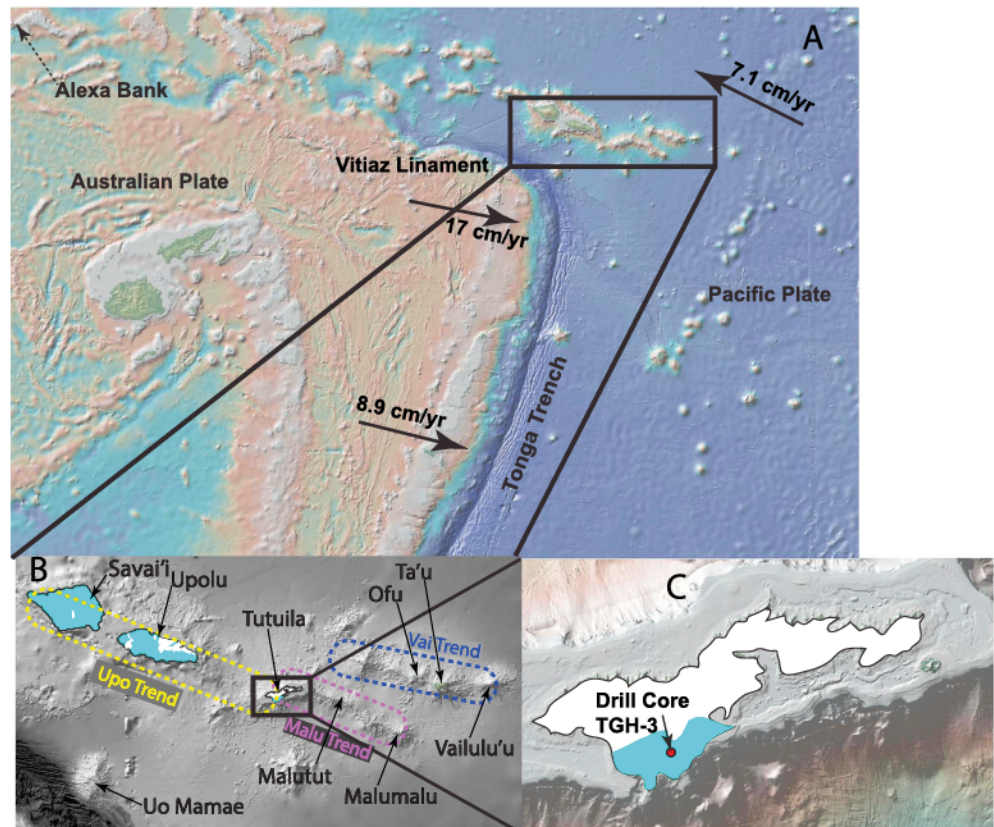


**Figure 1.** Regional (a), archipelago (b), and island (c) scale maps of the study area. Volcanic trends in the lower left panel are from Jackson et al. (2014). In (b) the cyan shading on the islands of Savai'i, Upolu, and Tutuila shows the extent of subaerially exposed rejuvenated volcanism (Konter & Jackson, 2012; Natland, 1980). In the same panel the Upo, Malu, and Vai trends are outlined in yellow, purple, and blue, respectively, which are defined by their distinct isotopic compositions (Jackson et al., 2014). Panel (c) shows the location of the geothermal exploration well (TGH-3) from which the samples in this study were taken. Plate velocities are from Bevis et al. (1995).

perform systematic major and trace element, radiogenic isotopic, and geochronologic analyses (including  $^{14}\text{C}$  and  $^{40}\text{Ar}/^{39}\text{Ar}$ ) of the Tutuila drill core. We find that the Tutuila drill core lava flow units sample several of the known mantle compositions in Samoa, including EM1 (enriched mantle 1) and dilute expressions of EM2 (enriched mantle 2), a depleted mantle (DM) component, and a primordial common component called FOZO (Focus Zone; Hart et al., 1992). We note (as detailed in Jackson et al., 2014) that, while Samoan lavas sample the most extreme EM2 lavas erupted in an oceanic setting, they do not exhibit true extreme endmember EM1, DM, HIMU (high “ $\mu$ ”), or common component FOZO material, but rather Samoan lavas have isotopic compositions that trend toward these endmembers. Therefore, when we refer to EM1, DM, and the FOZO component material sampled by Samoan lavas, the implication is that these lavas are sampling these components in diluted form.

The geochemical boundaries between the compositions identified in subaerial Tutuila basalts are abrupt and marked by the appearance of reef carbonates in the upper 150 m of the core and by muds and diamicts and/or volcanoclastic breccias deeper in the core. Critically, the Tutuila drill core captures the boundary between rejuvenated and shield stage lavas, which allows us to temporally constrain the onset of rejuvenated volcanism on Tutuila at the location of this drill core (rejuvenated volcanism on Tutuila is geographically limited to the southwest portion of the island where this core was drilled; see Figure 1) and the time elapsed between the termination of shield stage and the initiation of rejuvenated stage lavas.

Rejuvenated volcanism in the Samoan Islands has long been attributed to the juxtaposition of the Samoan Islands to the Tonga Trench (Konter & Jackson, 2012; Koppers et al., 2008, 2011; Natland, 1980; Wright & White, 1987). Therefore, establishing the timing of the onset of rejuvenated volcanism at Tutuila allows us



to evaluate a possible relationship between the approach of a Samoan volcano to the Tonga Trench and the onset of rejuvenated Samoan volcanism.

Recently, it has been proposed that oceanic volcanism can be triggered when ancient oceanic lithosphere flexes as it approaches subduction zones; the resulting volcanoes, called “petit spots,” were first identified outboard of the Japanese Trench (Hirano et al., 2001, 2006, 2008; Machida et al., 2015; Yamamoto et al., 2014). Magmas of similar tectonic origin and geochemistry have also been reported in late-stage lavas at Christmas Island, located ~150 km outboard of the Sunda Trench; at Christmas Island, the final, youngest (4.3 to 4.5 Ma) stage of volcanism caps an older (37 to 44 Ma) stage of volcanism on the island (Hoernle et al., 2011; Taneja et al., 2015). Hoernle et al. (2011) argue that the late-stage lavas at Christmas Island provide an example of a tectonic trigger (i.e., uplift as the island moved over the flexural bend as it approached the Java Trench) for late-stage volcanism at an ocean island volcano. Notably, a flexural model has also been suggested for generating rejuvenated volcanism at Hawai‘i, although the flexure at Hawai‘i is the result of lithospheric loading by the large volcanic edifices themselves and not subduction (Bianco et al., 2005). Konter and Jackson (2012) demonstrated that a tectonic trigger is a plausible mechanism for generating rejuvenated Samoan volcanism, based on the expected timing of Samoan rejuvenated volcanism as Samoan volcanoes approach the northern terminus of the Tonga Trench. The examination of rejuvenated volcanism at Tutuila presented here provides insight into the timing of the onset of rejuvenated volcanism in Samoa and whether it relates to the volcano’s approach to the northern terminus of the Tonga Trench. Here we also present geochemical evidence suggesting that Samoan rejuvenated lavas sample a similar enriched mantle reservoir to that sampled by other tectonically influenced, near-trench volcanoes in the western Pacific (such as the petit spot volcanoes near the Japanese Trench) and eastern Indian Oceans (such as late-stage Christmas Island volcanism, which has compositions that resemble petit spot lavas). We also examine the appearance of various geochemical components along the stratigraphy of the Tutuila drill core and compare this with the geochemical stratigraphy inferred for other Samoan volcanoes to develop a preliminary model for the geochemical evolution of a Samoan volcano.

## 2. Geologic Background

The Samoan Islands form an age-progressive volcanic hotspot track on the Pacific plate (Figure 1) that is anchored to the active eastern end at Vailulu‘u (Hart et al., 2004, 2000; Koppers et al., 2008, 2011; Sims et al., 2008; Staudigel et al., 2006). Like Hawai‘i—which has two *en echelon* volcanic lineaments, “Loa” and “Kea”—the eastern Samoan region has two *en echelon* volcanic lineaments, referred to as “Vai” and “Malu” (Koppers et al., 2011). Samoan volcanism extends as far west as Alexa Bank (23.4 Ma; Hart et al., 2004), and small groups of Cretaceous seamounts in the western Pacific are suggested to be related to the Samoan hotspot (Koppers et al., 2003).

The Samoan hotspot lies just outboard of the Tonga Trench: the island of Savai‘i, the largest Samoan Island, is presently ~130 km from the northern terminus of the Tonga Trench. At the northern terminus of the Tonga Trench, the Pacific plate tears and subducts beneath the Australian plate, while the northern portion of the plate continues westward. It is this unique tectonic setting that has been suggested to influence magmatism on the Samoan Islands (Hawkins & Natland, 1975; Natland, 1980), in particular the rejuvenated stage of volcanism (Hart et al., 2004; Konter & Jackson, 2012; Koppers et al., 2008). Shield stage volcanism in the Samoan Islands is related to a seismically imaged low-velocity conduit, or plume, beneath the hotspots (Chang et al., 2016; French & Romanowicz, 2015; Maguire et al., 2017), and Pacific plate motion over the plume results in a clear age progression of shield-stage volcanism at Samoa (Koppers et al., 2008, 2011). Konter and Jackson (2012) argue that the more recent veneer of rejuvenated volcanism in the western Samoan Islands (Savai‘i, Upolu, and Tutuila) is driven by regional tectonics as the Pacific plate flexes upward as it passes by the northern terminus of the Tonga Trench.

A significant fraction of the surface exposure of the two westernmost subaerially exposed volcanoes of the Samoa hotspot track, Savai‘i and Upolu (>99% and ~50%, respectively; Figure 1), is covered with a veneer of rejuvenated volcanism (Konter & Jackson, 2012; Natland & Turner, 1985; White, 1985). Of the Hawai‘ian volcanoes that display rejuvenated volcanism, the subaerial coverage by rejuvenated lavas is generally <6%. The two exceptions are Ni‘ihau and Kaua‘i, where rejuvenated lavas cover ~35% of the volcanoes subaerial extent (Clague & Sherrod, 2014; Garcia et al., 2010, 2016). Among Samoan volcanoes, rejuvenated

volcanism on Tutuila covers a much smaller fraction (~15%) of the subaerially exposed portion of the volcanic edifice than at Savai'i and Upolu and may indicate that rejuvenated volcanism on Tutuila initiated only recently (see section 4.1.) and is in an earlier stage of tectonically driven rejuvenated volcanism.

Lavas erupted at the Samoan hotspot sample five geochemical groups (Jackson et al., 2014): (1) EM2 (geochemically very radiogenic  $^{87}\text{Sr}/^{86}\text{Sr}$  and unradiogenic  $^{143}\text{Nd}/^{144}\text{Nd}$ ; intermediate Pb isotopic compositions); (2) relatively dilute EM1 (geochemically enriched  $^{87}\text{Sr}/^{86}\text{Sr}$  and  $^{143}\text{Nd}/^{144}\text{Nd}$ , unradiogenic Pb isotopic compositions); (3) dilute HIMU (pure HIMU represents highly radiogenic Pb isotopic compositions); (4) a primordial common component called Prevalent Mantle (Wörner et al., 1986; Zindler & Hart, 1986), FOZO, C (common; Hanan & Graham, 1996), or Primitive He Mantle (PHEM; Farley et al., 1992) that is characterized by having intermediate radiogenic isotopic compositions and  $^3\text{He}/^4\text{He} > 20 \text{ Ra}$ ; and (5) a component that trends toward DM (unradiogenic  $^{87}\text{Sr}/^{86}\text{Sr}$  and Pb isotopic compositions, radiogenic  $^{143}\text{Nd}/^{144}\text{Nd}$ ). Jackson et al. (2014) proposed that three of these geochemical compositions are expressed at the Samoan hotspot as three volcanic lineaments: the Upo (DM) volcanic trend, the Malu (EM2) volcanic trend, and the Vai (HIMU) volcanic trend that coincide with the En Echelon configuration of the seamount trail subtracks (Koppers et al., 2011; Workman et al., 2004; Figure 1). The three oldest islands (Savaii, Upolu, and Tutuila) are veneered by rejuvenated lavas with an EM1 composition. Using new data for the geochemical stratigraphy of Tutuila from the drill core, together with the inferred geochemical stratigraphy at other Samoan volcanoes, we propose a preliminary model for the geochemical evolution of Samoan shield volcanoes.

### 3. Methods

#### 3.1. Major and Trace Elements

Major and trace element concentrations were measured in 92 whole-rock basalt samples. Samples were selected for freshness while at the same time being representative of all igneous lithologies in the core and providing relatively even coverage across all depths in the core. For sections of the core that appeared altered, the least visibly altered portions of the lava flow were sampled. In preparation for analysis the samples were cut with a rock saw to avoid material that was in contact with the coring bit. After cutting from the core material, samples were then sanded with silicon carbide abrasive paper to remove any potential metal contaminants left behind by the saw blade. After sanding, the samples were crushed, and the freshest rock chips were picked under a binocular microscope to avoid visibly altered material. Finally, all samples were rinsed in deionized water to remove any surface contaminants from sanding or crushing. The samples were then analyzed at the Peter Hooper GeoAnalytical Lab at Washington State University for their major and trace element concentrations. The rock samples were powdered in an agate mortar, and the powders were then fused and analyzed for major element concentrations via X-ray fluorescence and trace elements via solution inductively coupled plasma mass spectrometry (ICP-MS; Knaack et al., 1994). Documented precision for  $\text{SiO}_2$ ,  $\text{Al}_2\text{O}_3$ ,  $\text{TiO}_2$ , and  $\text{P}_2\text{O}_5$  analyses is 0.2–0.7% ( $2\sigma$ ) of the amount present and 0.8–1.4% ( $2\sigma$ ) for  $\text{FeO}_T$ ,  $\text{MgO}$ ,  $\text{CaO}$ ,  $\text{Na}_2\text{O}$ ,  $\text{MnO}$ , and  $\text{K}_2\text{O}$  (Johnson et al., 1999); trace element ICP-MS analyses have a precision of 1.5–6.4% ( $2\sigma$ ; Knaack et al., 1994), except for Th (8%) and U (9%). Three United States Geological Survey (USGS) reference materials (BHVO-2, BCR-2, and G-2) were run as unknowns for major and trace elements with the Samoan basalt samples reported here (see Table S1 in the supporting information). For all three reference materials  $\text{SiO}_2$ ,  $\text{Al}_2\text{O}_3$ ,  $\text{MgO}$ ,  $\text{CaO}$ ,  $\text{Na}_2\text{O}$ ,  $\text{TiO}_2$ , and  $\text{K}_2\text{O}$  were within 2.2% of the preferred values from Jochum et al. (2015). Other elements analyzed by X-ray fluorescence— $\text{P}_2\text{O}_5$  (within 0.7 to 4.0%, depending on the USGS reference material),  $\text{FeO}_T$  (0.4 to 3.8%), and  $\text{MnO}$  (0.1 to 9.4%)—deviate more from Jochum et al.'s (2015) preferred values (see Table S1). Most trace element concentrations measured by ICP-MS were within 5% of the Jochum et al.'s (2015) preferred values for all three reference materials (Rb, Ba, U, Ta, La, Ce, Pb, Pr, Nd, Sr, Zr, Hf, Gd, Y, Er, Tm, Yb, and Lu), while the other elements (Cs, Th, Nb, Sm, Eu, Tb, Dy, Ho, and Sc) reproduced to within 10% of the Jochum et al. (2015) preferred values.

#### 3.2. Isotopes

A subset of 15 of the 92 samples analyzed for major and trace element concentrations was analyzed for  $^{87}\text{Sr}/^{86}\text{Sr}$ ,  $^{143}\text{Nd}/^{144}\text{Nd}$ , and Pb isotopic ratios. The samples selected for isotopic analyses were selected based upon the major and trace element data to span the wide range of major and trace element compositions encountered in the core. All six samples that were dated via  $^{40}\text{Ar}$ – $^{39}\text{Ar}$  (see section 3.4) were among those



selected for isotopic analysis. Rock chips selected for isotopic analyses were leached in 6N HCl at 90 °C prior to dissolution. Rock chips were dissolved in lieu of powders to avoid contamination from grinding equipment, which has been demonstrated to contribute significant Pb to samples (Takamasa & Nakai, 2009). Chemical separations were performed at Woods Hole Oceanographic Institution following the methods described in Hart and Blusztajn (2006). All isotopic measurements were made on the Thermo Scientific Neptune multicollector ICP-MS housed at Woods Hole Oceanographic Institution. The procedural blanks were 65, 10, and 50 pg for Sr, Nd, and Pb, respectively. Sr isotopic analyses were corrected for mass bias assuming  $^{86}\text{Sr}/^{88}\text{Sr}$  of 0.1194 and assuming the exponential law. Rb and Kr isobaric interferences were corrected using the method of Jackson and Hart (2006). Sr isotopic analyses were made over the course of two analytical sessions; repeat analyses of NBS 987 yielded average  $^{87}\text{Sr}/^{86}\text{Sr}$  ratios of 0.710334 ( $\pm 0.000018$ ,  $2\sigma$ ,  $n = 5$ ) and 0.710300 ( $\pm 0.000018$ ,  $2\sigma$ ,  $n = 3$ ) respectively, and samples were corrected for the offset between measured (in the same analytical session) and preferred (0.710240) values of the standard. Nd isotopes were corrected for mass bias by normalizing to  $^{146}\text{Nd}/^{144}\text{Nd} = 0.7219$  and assuming the exponential law; samples were corrected for the offset between the measured (in the same analytical session) and preferred JNdi-1 value of 0.512104 (Hamelin et al., 2011). Nd isotopes were also measured over the course of two analytical sessions; repeat analyses of JNdi-1 run over the course of two analytical session yielded average  $^{143}\text{Nd}/^{144}\text{Nd}$  ratios of 0.512090 ( $\pm 0.000016$ ,  $2\sigma$ ,  $n = 4$ ) and 0.512094 ( $\pm 0.000022$ ,  $2\sigma$ ,  $n = 3$ ), respectively. Pb isotopic compositions were corrected for mass bias on the instrument by Tl addition (SRM997), assuming a  $^{205}\text{Tl}/^{203}\text{Tl} = 2.38709$  and the exponential law (White et al., 2000); samples were corrected for the offset between the measured (in the same analytical session) and preferred NBS981 values of from Eisele et al. (2003) of 16.9409 ( $^{206}\text{Pb}/^{204}\text{Pb}$ ), 15.4976 ( $^{207}\text{Pb}/^{204}\text{Pb}$ ), and 36.7262 ( $^{208}\text{Pb}/^{204}\text{Pb}$ ). Pb isotopes were also measured over the course of two analytical sessions; repeat analyses of NBS981 run over the course of two analytical sessions yielded an average  $^{206}\text{Pb}/^{204}\text{Pb}$  of 16.9329 ( $\pm 0.0020$ ,  $2\sigma$ ,  $n = 4$ ),  $^{207}\text{Pb}/^{204}\text{Pb}$  of 15.4855 ( $\pm 0.0020$ ,  $2\sigma$ ,  $n = 4$ ),  $^{208}\text{Pb}/^{204}\text{Pb}$  of 36.6827 ( $\pm 0.0065$ ,  $2\sigma$ ,  $n = 7$ ) ratios for the first session and an average  $^{206}\text{Pb}/^{204}\text{Pb}$  of 16.9338 ( $\pm 0.0004$ ,  $2\sigma$ ,  $n = 3$ ),  $^{207}\text{Pb}/^{204}\text{Pb}$  of 15.4862 ( $\pm 0.0008$ ,  $2\sigma$ ,  $n = 7$ ),  $^{208}\text{Pb}/^{204}\text{Pb}$  of 36.6832 ( $\pm 0.0020$ ,  $2\sigma$ ,  $n = 7$ ) ratios for the second session.

Two aliquots of unleached USGS reference material BCR-2 powder were dissolved, chemically separated, and analyzed with the unknowns. The measured  $^{87}\text{Sr}/^{86}\text{Sr}$ ,  $^{143}\text{Nd}/^{144}\text{Nd}$ ,  $^{206}\text{Pb}/^{204}\text{Pb}$ ,  $^{207}\text{Pb}/^{204}\text{Pb}$ , and  $^{208}\text{Pb}/^{204}\text{Pb}$  ratios of the two BCR-2 aliquots agree within error with the values reported by Weis et al. (2006; see Table S1).

### 3.3. $^{14}\text{C}$ geochronology

Two reef carbonate units are present in the drill core (see section 4 below): the upper carbonate unit (located at 82.3 to 91.1 m depth) and the lower carbonate unit (135.9 to 150.3 m depth). Three carbonate samples from the stratigraphically higher carbonate unit (one sample from near the top and two from near the bottom of this unit) and one sample from the top of the stratigraphically lower carbonate unit were selected for  $^{14}\text{C}$  analyses. The four samples analyzed include a bivalve (*Wallucina fijiensis*), two corals (*Scleractinia*), and a second bivalve (species unknown). All are extremely fresh and show no evidence of alteration or thermal metamorphism (Figure S1). These four samples were analyzed for  $^{14}\text{C}$  using the W.M. Keck Carbon Cycle Mass Spectrometer located at the University of California Irvine. The samples provided ages with uncertainties  $<131$  years ( $2\sigma$ ; see Table S2). The radiocarbon ages were calculated using the Calib7.0.4 software (calib.qub.ac.uk/calib/) the Marine13 calibration curve (Reimer et al., 2013), and a  $\Delta R$  (the correction for the marine radiocarbon reservoir) value of  $+57 \pm 23$  (Phelan, 1999) was used as it is the published reservoir value geographically closest to the Tutuila drill core.

### 3.4. $^{40}\text{Ar}/^{39}\text{Ar}$ Geochronology

Basalt samples were prepared for analysis by sawing, crushing, and magnetic separation. Following separation, the samples were then irradiated for 6–7 hr in the TRIGA CLICIT nuclear reactor at Oregon State University.  $^{40}\text{Ar}/^{39}\text{Ar}$  measurements were made on six samples from the Tutuila drill core by incremental heating of basaltic groundmass separates on the multicollector ARGUS-VI mass spectrometer at Oregon State University using the methods detailed in Koppers et al. (2011) and Konrad et al. (2018). Ages are calculated as weighted means  $1/\sigma^2$  using the ArArCALC v2.7.0 software from Koppers (2002, available at earth-ref.org/ArArCALC). For the age calculations the Steiger and Jager (1977) decay constant

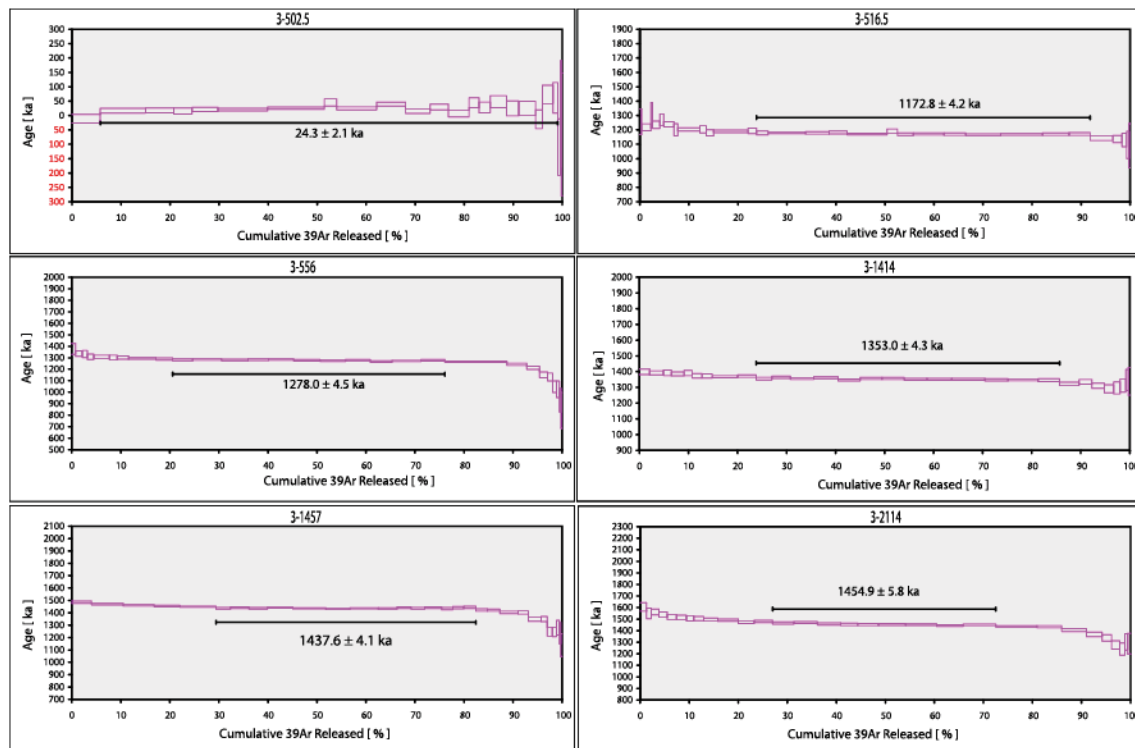


**Figure 2.** High-resolution incremental heating  $^{40}\text{Ar}/^{39}\text{Ar}$  age spectra for Tutuila drill core lavas dated in this study. Plots are arranged in depth order from shallowest to deepest. The  $^{40}\text{Ar}/^{39}\text{Ar}$  ages are weight age estimates with 95% confidence level errors including 0.3–0.5% standard deviations in the  $J$  value. Data can be found in Table S3.

( $5.530 \pm 0.097 \times 10^{-10}$ ) as corrected by Min et al. (2000) was used. Ages were normalized to a Fish Canyon Tuff sanidine standard using the preferred age of  $28.201 \pm 0.023$  Ma (Kuiper et al., 2008). All  $^{40}\text{Ar}/^{39}\text{Ar}$  data are of high quality, and age plateau plots can be found in Figure 2 and data can be found in Table S3.

## 4. Data and Observations

### 4.1. Physical and Geochronological Description

The Tutuila drill core was drilled from a surface elevation of 76.8 m above mean sea level to a total depth of 645.3 m or 568.5 m below mean sea level. All depths discussed will be in reference to the top of the well, not mean sea level. The drill core is preserved in the USGS Core Research Center at Denver, CO (Core number R286). Below we provide a lithological and petrological overview of the drill core as well as a description of the major boundaries and, where available, their ages. A detailed core log is reported elsewhere (my.usgs.gov/crcwc), and images of the entire drill core are available online (escholarship.org/uc/item/6gg6p61w).

The uppermost 4.3 m of the hole was rotary drilled and not recovered. From 4.3 to 78.3 m, the recovered core is basaltic lava flows with abundant small (<1 mm) olivine phenocrysts and occasional small (< 2 cm) peridotite xenoliths. The lavas have variable vesicularity ranging from <5% to 60% vesicularity (scoriaceous). From 78.3 to 82.3 m the recovered material is hard to friable, brownish red to black volcanoclastic deposits.

The section of drill core recovered from 82.3 to 91.1 m is carbonate reef material composed of individual coral fragments (with individual reef units up to 75 cm thick) interlayered with varying abundances of brecciated corals and carbonate mud. The core transitions from grain stone to float stone and at the base is frame stone. This suggests that this carbonate reef interval represents a relatively shallow portion of an active reef. A fully intact articulated bivalve (*W. fijiensis*) was taken from 83.6-m depth (near the top of the upper carbonate unit) for radiocarbon dating. This sample yielded a calibrated median  $^{14}\text{C}$  age of  $4,438 \pm 102$  years before present (BP), and this age provides a maximum age for the lavas that lie above this carbonate unit. Two carbonate samples, a coral (*Scleractinia*) and a bivalve (species unknown), were taken from near the base of the upper carbonate unit, at 90.1 and 90.8 m depth, respectively, and yielded calibrated median



$^{14}\text{C}$  ages of  $6,997 \pm 125$  and  $7,128 \pm 114$  years BP: these two ages overlap within error and provide a minimum age for the lavas located between the upper and lower carbonate units of the drill core. Located at depths of approximately 7 to 14 m below present-day sea level, the bivalve (at 4,438 years BP) and the coral and shell (6,997 and 7,128 years BP) were deposited at depths roughly corresponding to paleo sea level in the Pacific at the times recorded by the  $^{14}\text{C}$  ages (Bard et al., 1996). This is consistent with the presence of the bivalve *W. fijiensis* in the upper carbonate unit, as this species typically lives in water depths between 0 and 15 m (Glover & Taylor, 2001).

From 91.1 to 135.9 m the drill core is basaltic lava flows with abundant small (<1 mm) olivine phenocrysts and occasional small (<2 cm) peridotite xenoliths. The lavas have variable vesicularity ranging from <5% vesicles to scoracious. While the lithology does not vary greatly from 91.1- to 135.9-m depth, approximately 65% of this depth interval consists of angular basaltic rubble (>5-cm diameter) that is visually similar to the intermittent unfractured sections of basalt in this depth interval. It is difficult to discern if the rubbly nature of some portions of this depth interval is the result of the drilling or is representative of highly fractured sections of lava.

A second, lower carbonate unit is found at 135.9 to 150.3 m and is composed of white to dark gray carbonate muds with brecciated corals and carbonate shell clasts. This carbonate section contains more carbonate mud, and significantly less brecciated coral, than the stratigraphically higher carbonate unit. This carbonate unit contains pack stones (with rounded coral cobbles) and mudstones, indicative of a deeper fore reef environment. A clast of coral from 138.1 m, taken from near the top of the lower coral unit, yielded a  $^{14}\text{C}$  median age of  $10,385 \pm 131$  years BP. This depth corresponds to a depth of approximately 61 m below current sea level, which roughly corresponds to ~15-m depth below estimates of paleo sea level at 10,300 years BP (Bard et al., 1996). However, this observation is consistent with a fore reef interpretation for the lower carbonate unit, as the fore reef would form at relatively greater depth than paleo sea level.

This lower carbonate unit lies above 7.1 m of moderately weathered aphanitic basalt flows (150.3- to 157.2-m depth). A sample from this depth section (153.2-m depth) in the drill core was dated by  $^{40}\text{Ar}/^{39}\text{Ar}$  to have an age of  $24.3 \pm 2.1$  ka, consistent with a young, rejuvenated volcanic origin, and in section 4.4, we show that these lavas have rejuvenated isotopic characteristics. All basalts erupted above 157.2-m depth will be referred to as rejuvenated lavas, as the shield-building basalt sampled at 157.4-m depth has an age of  $1,172.8 \pm 4.2$  ka (see below). This interpretation is consistent with a drill core being situated atop the Leone rejuvenated lava series on Tutuila (Natland, 1980; Stearns, 1944).

The material between 157.2 and 167.8 m is primarily composed of siliciclastic sediments (clay, silt, sand, and volcanic clasts) that lie unconformably on top of deeper basalt flows and is shown as a brown layer in Figure 3. Referred to as the “upper breccia and diamict unit” in Figure 3, this unit represents an unconformity between the shield and rejuvenated stages of volcanism. The depth from 157.2 to 163.4 m consists of a poorly lithified breccia composed of ~65% angular basaltic clasts (1–5 cm) and 35% yellow-brown mud. The basaltic sample (3–516.5) from the top of this unit was dated by  $^{40}\text{Ar}/^{39}\text{Ar}$  and yielded an age of  $1,172.8 \pm 4.2$  ka (Figure 3). However, it is challenging to determine whether this sample is from a lava flow or is a cobble based on the context of an 8.5-cm drill core (a second sample from within this diamict may also be a cobble [3–526.5]). Between 163.4 and 165.4 m, the recovered drill core is unlithified friable reddish-brown to brown mud with <30% silt to sand-sized particles. The deepest portion of this sedimentary sequence (165.4 to 167.8) is a poorly lithified friable breccia composed of ~50% angular basaltic clasts (0.5–4 cm) and 50% yellow-brown mud and silt.

The depth section from 167.8 to 431.0 m, which lies immediately below the shield-rejuvenated unconformity and spans 263.2 m, consists primarily of basaltic lava flows (60%) with interlayered volcanoclastic material (30%; dominantly breccias) and occasional lapilli tuffs (10%). The basalts in this section of the core are dominantly aphanitic, with occasional flows with small (<1 mm) olivine phenocrysts that have been completely iddingsitized and one flow with large (up to 3 cm) moderately altered plagioclase phenocrysts. The matrix of the volcanoclastic breccias and the tuffs is generally highly altered, and include secondary carbonate, consistent with a submarine volcanic origin (similar volcanic morphologies are identified throughout the shield stages sampled in the core). One lava flow sample from near the top (169.5 m) and one sample from the bottom (431.0 m) of this section were dated by  $^{40}\text{Ar}/^{39}\text{Ar}$  to  $1,278 \pm 4.5$  and  $1,353 \pm 4.3$  ka, respectively. Thus, the lavas from this depth section, representing nearly 41% of the drill core's depth, span only

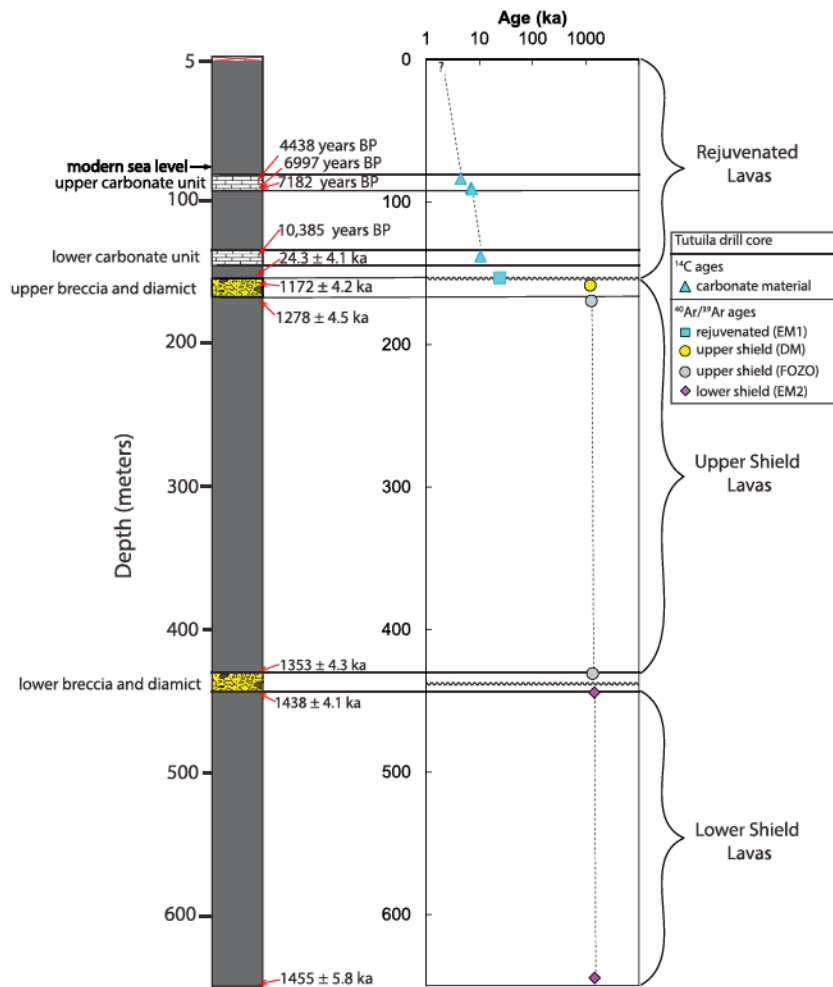


**Figure 3.** Simplified stratigraphic column of the drill core. An age-depth relationship is also shown for age-dated samples in the Tutuila drill core. Cyan triangles represent carbonate material dated by  $^{14}\text{C}$ , while the other symbols represent  $^{40}\text{Ar}/^{39}\text{Ar}$  ages of lavas. Symbol colors correspond to sample depth (cyan is rejuvenated, gray and yellow are upper shield, and pink is lower shield), which relates to the geochemical classification of the lavas (EM1, FOZO, DM, and EM2, respectively). A detailed core log for this drill core is available at [my.usgs.gov/crcwc](http://my.usgs.gov/crcwc). EM = enriched mantle; FOZO = focus zone; DM = depleted mantle.

~75,000 years of volcanic history. The basalts from the upper breccia and diamict unit and the lavas, between 167.8 and 432.2 m, will be referred to as the upper shield lavas (which will be shown in section 4.4 to have radiogenic isotopic compositions that are consistent with the primordial common FOZO component previously identified in Samoa (Farley et al., 1992; Jackson et al., 2014; Workman et al., 2004), as well as five lavas with DM characteristics).

Between 432.2 and 443.9 m, spanning 12.9 m, the recovered drill core is composed of volcanoclastic breccia that lies on top of a (~0.9 m) diamict section (and is shown as a yellow layer in Figure 3, labeled “lower breccia and diamict” unit). Basalts taken from immediately above ( $1,353 \pm 4.3$  ka at 431.0 m depth) and below ( $1,438 \pm 4.1$  ka at 444.1 m) this breccia and diamict unit span an age range of ~85 ka. Thus, the lower breccia and diamict unit represents a relatively short volcanic hiatus between the 263.2-m-thick basalt depth section above and the 201.2-m-thick basalt depth section below.

From 443.9 to 645.3 m, spanning 201.2 m, the drill core is predominantly basalt flows (~70%) with inter-layered highly altered (30%) volcanoclastic units (dominantly breccias). The basalts in this section range from minimally to moderately altered and frequently have clinopyroxene (~75%) and occasionally (20%) have olivine phenocrysts. Phenocrysts range from <1 mm to ~1 cm in size. One lava from near the top of this section



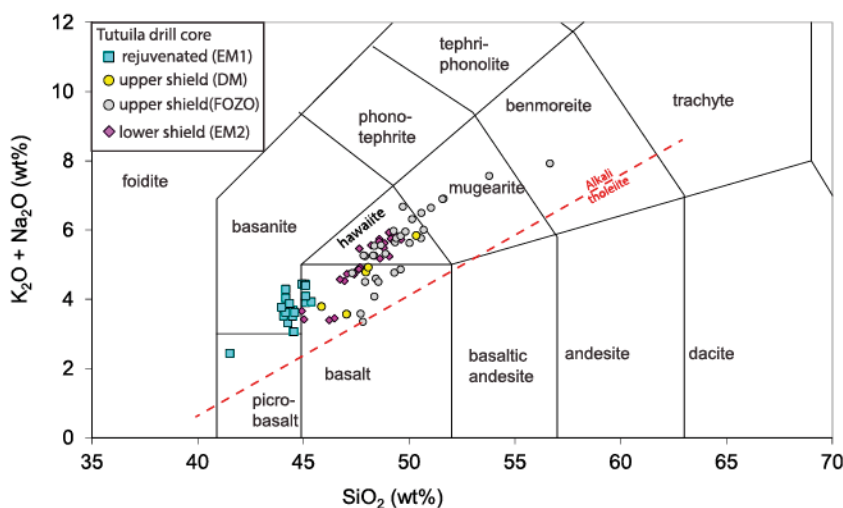


**Figure 4.** Total alkali versus silica plot of the analyzed Tutuila drill core samples. Rock-type classifications are based on le Maitre (2002). Symbol colors as in Figure 3. The alkali-tholeiite line is from Macdonald and Katsura (1964). EM = enriched mantle; FOZO = focus zone; DM = depleted mantle.

of the drill core (444.1 m) was dated by  $^{40}\text{Ar}/^{39}\text{Ar}$  to  $1,438 \pm 4.1$  ka. Additionally, a sample from near the bottom of the drill core (644.4 m) was dated to  $1,455 \pm 5.8$  ka, and this sample is a portion of the deepest lava flow that extends to the completion depth of the well (645.3 m). The difference in ages between the top and bottom of this 201.2 m section is only  $\sim 17$  ka. The lowermost 201.2 m of the drill core will be referred to as the lower shield lavas (and we show in section 4.4 that these lavas have EM2 characteristics).

#### 4.2. Major Elements

Major and trace elements for the 92 samples analyzed in this study are presented in Table S4. All 92 lavas are generally fresh with a few outliers, as shown in Figure S2. On a total alkali versus silica diagram (Figure 4), the rejuvenated lavas from the Tutuila drill core plot in the fields defined by basalts and basanites and all lavas are alkalic or transitional. However, the deepest lava in the rejuvenated series is a picrobasalt (sample 3-502.5). The upper shield lavas have compositions that include basalts, hawaiites, mugearites, and a single benmoreite. The lower shield lavas are composed of basalts and hawaiites, as well as one basanite. The silica content of the rejuvenated lavas is generally lower than the shield lavas. The rejuvenated lavas show relatively little variability in silica content ( $39.6$  to  $45.4$  wt. %; Table S4). The shield lavas show a greater variability in total alkali content, and they generally have higher total alkali content than the rejuvenated lavas.

Whole rock major elements are plotted against MgO concentrations for the samples analyzed in this study in Figure 5. Previously published major element data from the Samoan hotspot chain are also plotted in Figure 5 (gray symbols represent shield lavas, and black symbols represent rejuvenated lavas). In  $\text{SiO}_2$  versus MgO (Figure 5) space, the lavas from this study fall within the range of compositions previously observed on Tutuila. The rejuvenated lavas from the Tutuila drill core tend to plot with rejuvenated lavas from other Samoan Islands in Figure 5. While Samoan rejuvenated lavas overlap with shield lavas, the rejuvenated lavas do not extend to the highly evolved compositions observed in the shield lavas. In the plot of CaO versus MgO (Figure 5), the upper shield lavas in the drill core trend to low MgO and low CaO, while the rejuvenated and lower shield lavas from the drill core do not exhibit such evolved compositions. Some of the upper shield lavas from the drill core trend toward the Tutuila trachytes analyzed by Natland (1980), who suggested that late shield lavas in Samoa can include more evolved compositions than earlier shield lavas. The upper shield lavas extend to higher  $\text{Na}_2\text{O}$  and  $\text{P}_2\text{O}_5$  contents (two elements that are generally incompatible during magmatic evolution) than other lavas from Tutuila. In the plots of  $\text{TiO}_2$  (and  $\text{FeO}_T$ ) versus MgO, there is a sharp decrease in  $\text{TiO}_2$  (or  $\text{FeO}_T$ ) with decreasing MgO, and this occurs at MgO concentrations less than  $\sim 5\%$ , suggesting a role for titanomagnetite crystallization.

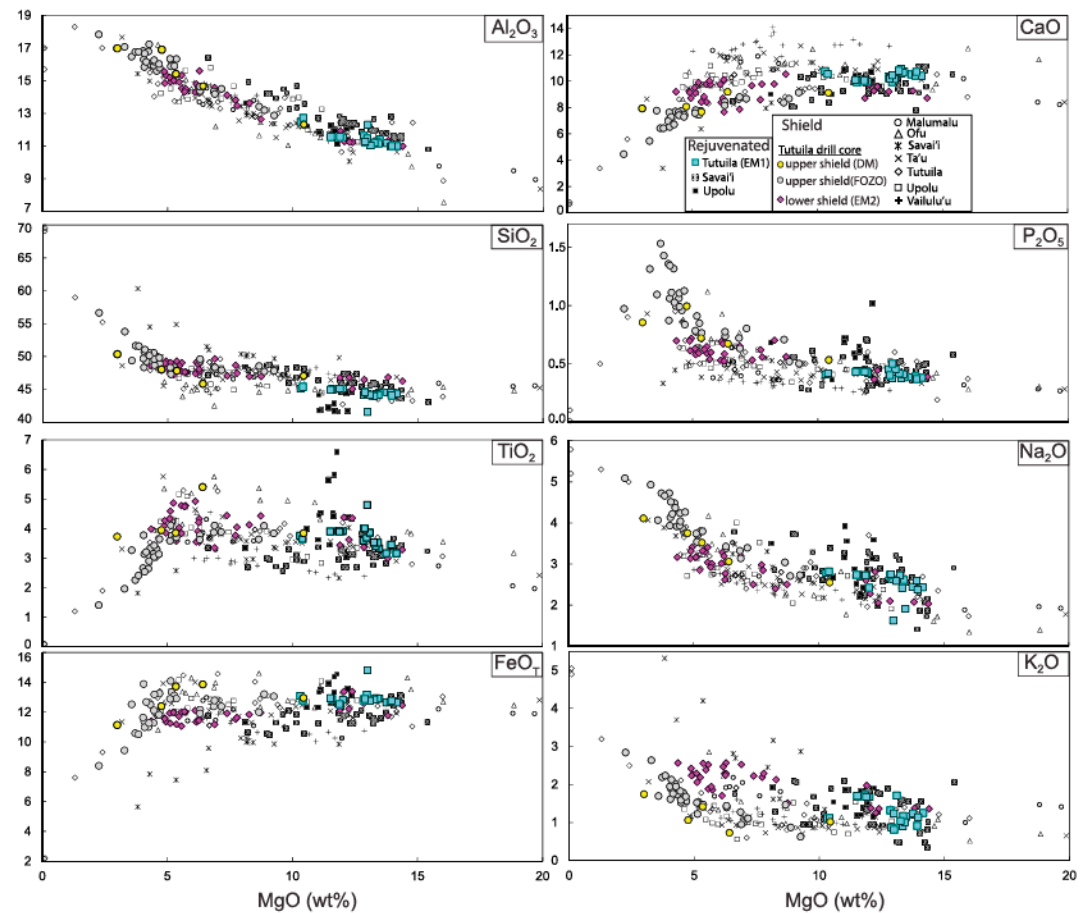


**Figure 5.** MgO versus major element oxide plots for samples examined in this study. All data are in weight percent. Previously published background data (black [rejuvenated lavas] and gray [shield lavas] symbols) were taken from Hawkins & Natland (1975), Natland (1980), and Natland and Turner (1985), Wright and White (1987), Workman et al. (2004), Jackson et al. (2007, 2010), Konter and Jackson (2012), and Hart and Jackson (2014). Symbol colors as in Figure 3. EM = enriched mantle; FOZO = focus zone; DM = depleted mantle.

#### 4.3. Trace Elements

The upper and lower shield lavas as well as the rejuvenated lavas have geochemically distinct trace element ratios (Figure 6). The upper shield lavas have lower Nb/Zr ratios (0.097 to 0.131) and do not overlap with the rejuvenated or lower shield lavas (0.147 to 0.196). Similarly, there is no overlap in Zr/Th ratios between the upper shield lavas (71.8–101) and the rejuvenated (46.5–68.9) or lower shield lavas (35.1–56.7). La/Yb ratios are also useful for distinguishing between the upper and lower shield lavas; the upper shield lavas have generally lower La/Yb ratios (12.7 to 21.1), while the lower shield lavas have higher La/Yb (20.2 to 39.1) (Figure 6). Thus, Nb/Zr, La/Yb, and Zr/Th ratios are useful for distinguishing between lower and upper shield lavas and demonstrate that there is a systematic shift in trace element geochemistry across the observed physical boundary (i.e., the lower volcanic breccia and diamict unit from 432.2- to 443.9-m depth) separating the upper and lower shield lavas.

Rejuvenated lavas from Savai'i, Upolu, and Tutuila are enriched in Ba relative to shield stage lavas (Jackson et al., 2010; Konter & Jackson, 2012; Workman et al., 2004), and Ba/Th ratios have been used to distinguish rejuvenated lavas (high Ba/Th) from shield-stage lavas (low Ba/Th) erupted at the Samoan hotspot (Jackson et al., 2010; Konter & Jackson, 2012; Workman et al., 2004). Figure 6 shows a clear distinction between the higher Ba/Th of the rejuvenated lavas (94.2 to 156.8) and the lower Ba/Th (40.4 to 72.1) of the shield lavas from the drill core. Thus, Ba/Th shows a systematic shift across the observed physical boundary (i.e., the breccia and diamict unit from 157.2 and 167.8 m depth) that separates the rejuvenated lavas above from



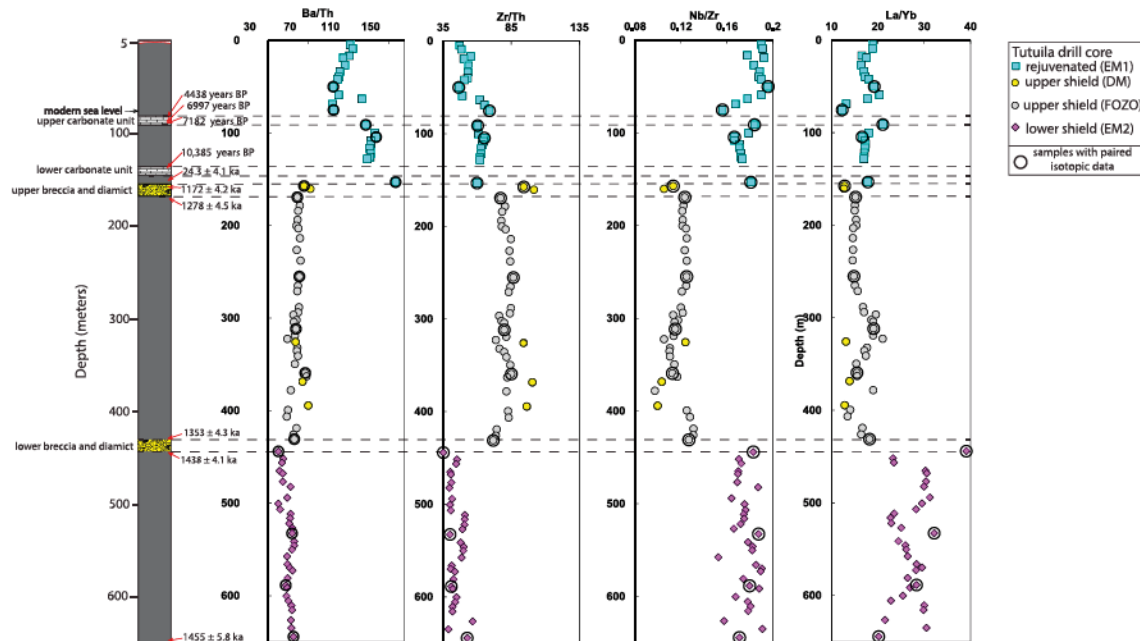


**Figure 6.** Trace element ratios versus depth in the core. Data can be found in Table S4. Samples circled in black were analyzed for radiogenic isotopes (see Figure 8). Ages on the stratigraphic column were obtained by  $^{14}\text{C}$  (samples younger than 11 ka) and  $^{40}\text{Ar}/^{39}\text{Ar}$  (samples older than 24 ka). Symbol colors as in Figure 3.

the shield lavas below (Figure 6). We note that Ba can be fluid mobile during alteration; however, these lavas show little evidence for significant Ba loss (Figure S2).

Jackson et al. (2014) identified five geochemical groups within the Samoan plume based on Pb isotopic ratios, and here we use relatively unevolved lavas ( $\text{MgO} > 5 \text{ wt.}\%$ ) from endmember volcanoes from these geochemical groups to generate representative fields for each group in trace element space: the Samoan EM1 field (defined by rejuvenated lavas from Savai'i and Upolu), the Samoan EM2 field (defined by EM2 lavas from the eastern Samoan volcanoes of Malumalu and Malutut), the Samoan HIMU field (defined by HIMU lavas from Ofu and Ta'u), the Samoan DM field (defined by DM lavas from Upolu and Alexa), and the Samoan primordial common component FOZO field, which is defined by Samoan lavas with  $^3\text{He}/^4\text{He} > 20 \text{ Ra}$  (Jackson et al., 2014). A plot of Zr/Th versus Ba/Th (Figure 7) shows the data from the Tutuila drill core in the context of fields for the different Samoan geochemical groups and demonstrates that trace element ratios are effective in (1) resolving rejuvenated lavas from shield lavas and (2) resolving the different geochemical groups identified in shield stage lavas, including Samoan EM2, DM, and FOZO (and HIMU) components. In Ba/Th versus Zr/Th space, the rejuvenated lavas from the drill core generally plot within the Samoan EM1 field (though the new data for Tutuila rejuvenated lavas suggest that the field for rejuvenated lavas should be expanded); much of the upper shield lavas span the FOZO and HIMU fields (which overlap in this trace element space), and a small subset of the upper shield series lavas—consisting of just five samples—plot within or near a Samoan DM field and we term these lavas “upper shield DM lavas” (this DM field is not the depleted MORB mantle but rather is the depleted component within the Samoan plume). The lower shield lavas from the drill core plot in the EM2 field.

#### 4.4. Radiogenic Isotopes

Consistent with their EM2 pedigree inferred from trace element ratios in Figure 7, the lower shield lavas have  $^{87}\text{Sr}/^{86}\text{Sr}$  ratios that are significantly geochemically enriched (0.706304–0.707734;  $n = 4$ ) relative to the other lavas in the Tutuila drill core (0.704978–0.705443;  $n = 11$ ; Figure 8). Therefore, the  $^{87}\text{Sr}/^{86}\text{Sr}$  ratios of the lower shield lavas are consistent with the enriched  $^{87}\text{Sr}/^{86}\text{Sr}$  ratios Farley et al. (1992) reported in lavas from the Masfau section on Tutuila (0.70583–0.70742). Similarly, the lower shield lavas have  $^{143}\text{Nd}/^{144}\text{Nd}$  ratios (0.512602–0.512661;  $n = 4$ ) that are significantly lower than the rest of the drill core and overlap with compositions observed in the Masfau section (0.51264–0.51272). The rejuvenated lavas generally have the

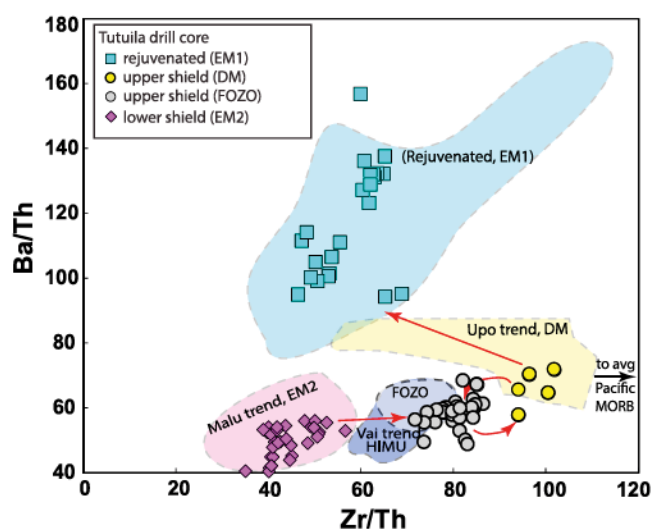


**Figure 7.** Ba/Th versus Zr/Th is plotted for all samples analyzed in this study. Data can be found in Table S4. The red arrows show compositional evolution of the lavas through time, starting with the lower shield lavas (EM2), the progressing to upper shield lavas (which cycle between volumetrically dominant FOZO lavas and intermingled DM lavas), and finally the rejuvénated lavas (EM1) in the shallowest portion of the drill core. The data fields are defined using published data (Hart & Jackson, 2014; Jackson et al., 2007, 2010; Kontar & Jackson, 2012; Workman et al., 2004): Lavas from the literature were filtered such that highly fractionated lavas ( $\text{MgO} < 5 \text{ wt.}\%$ ) are not shown, and only data obtained by ICP-MS are included. The fields in this figure are defined by samples that have been determined to be associated with isotopic groups (i.e., EM1, EM2, HIMU, FOZO, and DM) as discussed in Jackson et al. (2014). The cyan field is derived from previously published rejuvénated lavas from the Savai'i and Upolu. The yellow field is derived from previously published DM shield lavas from Upolu (Workman et al., 2004) and Alexa seamount (Hart et al., 2004). The gray field (the FOZO common component) encompasses all Samoan lavas with  $^3\text{He}/^4\text{He} > 20$ . The dark blue field encompasses previously published lavas with (dilute) HIMU radiogenic isotopic signatures from Ofu and Ta'u volcanoes. The pink field encompasses previously published lavas with EM2 radiogenic isotopic signatures from Malumalu and Malutut seamounts. Sample U10 (from Upolu) has trace element characteristics similar to rejuvénated lavas but isotopic compositions consistent with shield volcanism. However, its field relationships are not reported and it is not shown here. The average Pacific MORB plotted is the average of EPR data as compiled by Gale et al. (2013). EM = enriched mantle; FOZO = focus zone; DM = depleted mantle.

omy.) Moving stratigraphically upward, a lava (sample 3–516.5 [157-m depth]) sampled from within the upper breccia and diamict unit has a DM isotopic composition like that observed in lavas from other Samoan volcanoes with DM signatures (Figure 9), and the trace element composition of this lava (including elevated Zr/Th) plots in the field defined by Samoan lavas with DM signatures (Figures 6 and 7). Four additional lavas from the upper shield, including a second lava from the upper diamict and breccia unit (sample 3–526.5 [160 mbsf]), have incompatible trace element compositions similar to sample 3–516.5 (Figures 6 and 7), consistent with a Samoan DM designation. These five Samoan DM lavas are found scattered throughout the upper shield (see Figure 6), interbedded with Samoan FOZO lavas, indicating that the Samoan DM lavas erupted in concert with lavas with FOZO characteristics that constitute the bulk of the upper shield stage (the occasional sampling of DM isotopic compositions within the otherwise FOZO upper shield stage is represented by the red circling arrows between blue and yellow symbols in Figures 7 and 9). Following an ~1,150-ka volcanic hiatus, rejuvénated lavas with EM1 isotopic signatures (Figure 9) and trace element signatures similar to other Samoan rejuvénated lavas (Figure 7) appear in the drill core at 24.3 ka, together with the deposition of two Holocene reef carbonate units.

lowest Pb isotopic ratios, but they overlap with the subset of shield lavas with the least radiogenic  $^{207}\text{Pb}/^{204}\text{Pb}$  and  $^{208}\text{Pb}/^{204}\text{Pb}$ . In contrast, the lower shield lavas have the highest Pb-isotopic ratios and do not overlap with the rejuvénated or upper shield lavas in any isotopic space (Figure 8).

Five geochemical groups were identified in Samoan hotspot lavas based on radiogenic isotopes (Jackson et al., 2014), and the lavas from the Tutuila drill core sample much of this geochemical variability. In multi-isotopic spaces the lower shield lavas plot within the Samoan EM2 field defined in Jackson et al. (2014; Figure 9). The upper shield lavas generally plot within Samoan FOZO field. The shallowest shield lava (a cobble hosted within the upper breccia and diamict unit) trends into the Samoan DM field in all radiogenic isotopic spaces (Figure 9). In all but  $^{143}\text{Nd}/^{144}\text{Nd}$  versus  $^{87}\text{Sr}/^{86}\text{Sr}$  isotopic space, the rejuvénated lavas from the drill core generally plot within or near the field defined by previously analyzed Samoan rejuvénated lavas, and one rejuvénated lava is shifted toward the Samoan DM field. However, given their young age following a protracted volcanic hiatus, and the shift in composition that is consistent with rejuvénated lavas (e.g., high Ba/Th, low  $^{206}\text{Pb}/^{204}\text{Pb}$ , etc.), we suggest that the compositional field for Samoan rejuvénated lavas should be expanded to include these rejuvénated lavas from the Tutuila drill core. Expanding the Samoan rejuvénated field boundary seems particularly appropriate given that no rejuvénated lavas from Tutuila have been previously characterized for both radiogenic isotopes and trace elements, so the rejuvénated field shown in Figure 9 consists of rejuvénated lavas from Upolu and Savai'i and no rejuvénated lavas from Tutuila.

Together, radiogenic isotopic measurements (Figures 8 and 9) and incompatible trace element ratios (Figures 6 and 7) provide insights into the geochemical evolution of Tutuila. The lower shield lavas from the Tutuila drill core have EM2 isotopic (Figure 9) and trace element (Figure 7) compositions similar to those previously observed in the Tutuila Masefau section (Farley et al., 1992; Workman et al., 2004) and lavas from other Samoan volcanoes with EM2 signatures (Jackson et al., 2014). Following a ~85-ka hiatus in volcanism, marked by deposition of diamict, the Tutuila volcano began to erupt the upper shield lavas dominated by lava flows with isotopic (Figure 9) and trace element (Figure 7) compositions similar to lavas from other Samoan volcanoes that have a high  $^3\text{He}/^4\text{He}$  FOZO component. (Unfortunately, none of the drill core samples that overlap with the high  $^3\text{He}/^4\text{He}$  region contains glass or olivine phenocrysts suitable for  $^3\text{He}/^4\text{He}$  analysis to confirm a FOZO taxonomy.)



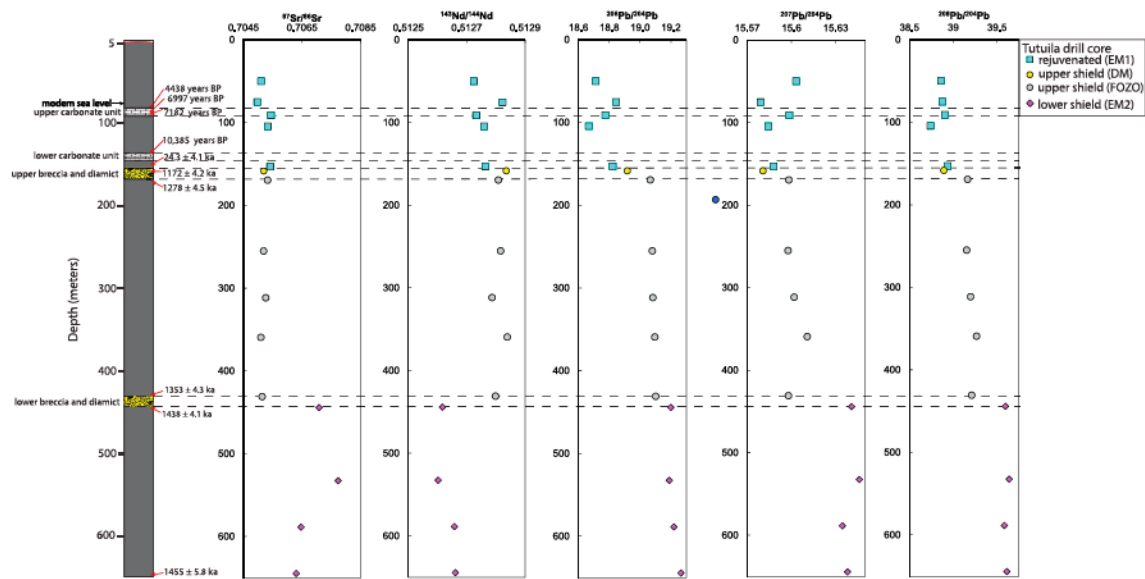


**Figure 8.** Depth versus heavy radiogenic isotopic compositions for the 15 lavas analyzed in this study. Ages on the stratigraphic column to the left were obtained by  $^{14}\text{C}$  (samples younger than 11 ka) and  $^{40}\text{Ar}/^{39}\text{Ar}$  (samples older than 24 ka). Data can be found in Table S4. Symbol colors as in Figure 3. EM = enriched mantle; FOZO = focus zone; DM = depleted mantle.

## 5. Discussion

### 5.1. Geochemical Evolution of Samoan Volcanoes

In ~650 m of volcanic stratigraphy from Tutuila, the drill core hosts lavas that have fingerprints of four of the five Samoan mantle isotopic groups observed at the Samoan hotspot: EM1, EM2, DM, and FOZO (but not HIMU). Critically, the isotopic compositions observed in the Tutuila drill core exhibit a clear temporal evolution: the deepest shield lavas have an EM2 composition, followed stratigraphically by upper shield lavas with Samoan FOZO compositions interlayered with Samoan DM composition lavas. Following an ~1.1-Myr hiatus, the shield lavas are capped by EM1 rejuvenated lavas (Figure 8).

Based on the geochemistry observed in the Tutuila drill core, we propose a generalized model for the geochemical evolution of a Samoan hotspot volcano. The main shield stage of volcanism produces lavas with EM2, FOZO (and, unlike Tutuila, some Samoan volcanoes erupt dilute HIMU compositions concurrently with, or in lieu of, FOZO-type lavas), and DM isotopic composition lavas (but DM compositions are observed only in the later upper shield stage, as observed on Tutuila). The final stage in a Samoan volcano's evolution is a cap of EM1 rejuvenated lavas following an ~1.1-Myr hiatus in volcanism. However, it is important to note that this model is based on a ~650-m drill core, which represents <10% of the modern vertical extent of one Samoan volcano. An important question is whether this geochemical progression is typical of other volcanoes at the Samoan hotspot, so we turn to subaerial and limited submarine sampling of other Samoan volcanoes to address this question and graphically summarize the available geochemical stratigraphy at each volcano in Figure S4.

We evaluate this model by first examining the older islands of the western portion of the Samoan hotspot (Savai'i and Upolu). At ~3,200 mbsl (meters below sea level), the deepest lavas dredged (dredge DR115) from Savai'i have extreme EM2 isotopic compositions (Jackson et al., 2007; Figure S4) and ages of 4.98 to 5.29 Ma (Koppers et al., 2011). Moving stratigraphically upward, two dredges between 2,660 (dredge DR118) and 2,560 (dredge DR128) mbsl returned lavas with EM2 signatures (Jackson et al., 2007): the age of the former dredge is unknown, and the latter has an age of 4.80 Ma (Koppers et al., 2011). Two lavas dredged (dredge DR114) from slightly higher on the flank of Savai'i (2490 mbsl), with an age of 4.24 Ma (Koppers et al., 2011), have dilute HIMU isotopic compositions with relatively high  $^3\text{He}/^4\text{He}$  (18.6 Ra; Jackson et al., 2010). However, the ~2,500 m of volcanic stratigraphy to sea level remains unsampled. The subaerial sampling of Savai'i has exclusively yielded samples with EM1 isotopic compositions associated with the rejuvenated lavas that have almost completely resurfaced the island (Konter & Jackson, 2012; Koppers et al.,

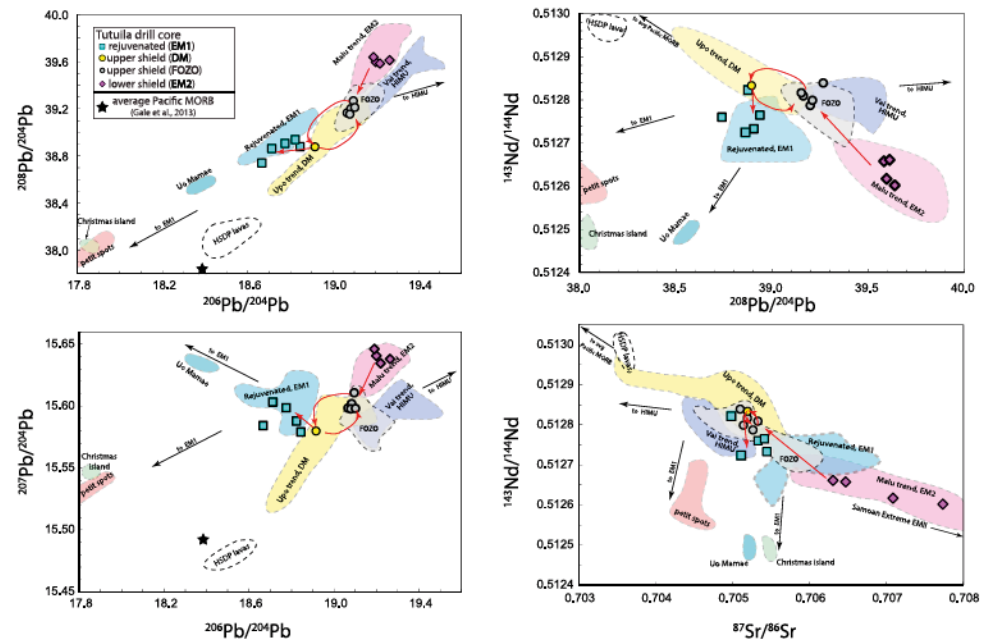


**Figure 9.** Radiogenic isotopic compositions for lavas analyzed in this study. The red arrows show compositional evolution of the lavas through time, starting with the lower shield lavas (EM2), the progressing to upper shield lavas (which cycle between volumetrically dominant FOZO lavas and intermingled DM lavas), and finally the rejuvenated lavas (EM1) in the shallowest portion of the drill core. The Samoan fields are defined by samples that have been determined to have isotopic endmember compositions as discussed in Jackson et al. (2014): the cyan field is derived from previously published rejuvenated lavas from the Savai'i and Upolu; the yellow field is derived from previously published DM shield lavas from Upolu (Workman et al., 2004), Tutuila Pago, and Alexa seamount (Hart et al., 2004); the gray field (FOZO) encompasses all Samoan lavas with  $^3\text{He}/^4\text{He} > 20$ ; the dark blue field encompasses previously published lavas with (dilute) HIMU radiogenic isotopic signatures from Ofu, Ta'u, Tamai'i, Soso, and Tupito volcanoes; the pink field encompasses previously published lavas with EM2 radiogenic isotopic signatures from Malumalu, Malutut, Tutuila Masefau, and Tulaga seamounts. The Christmas Island field encompasses the upper volcanic series (UVS, published in Hoernle et al., 2011), which we refer to as Christmas Island rejuvenated lavas. The petit spot field encompasses the petit spot lavas from outboard of the Japan Trench published by Machida et al. (2009). Uo Mamae lavas were previously published by Regelous et al. (2008) and Falloon et al. (2007). Christmas Island, petit spot lavas outboard of the Japan Trench, and Samoan rejuvenated lavas (together with Uo Mamae) sample different EM1 domains (all characterized by having low  $^{143}\text{Nd}/^{144}\text{Nd}$  at a given  $^{87}\text{Sr}/^{86}\text{Sr}$  and high  $^{208}\text{Pb}/^{204}\text{Pb}$  at a given  $^{206}\text{Pb}/^{204}\text{Pb}$ ), and the different EM1 reservoirs sampled by tectonically induced volcanism are shown with black arrows. The HSDP field encompasses the lavas published in Eisele et al. (2003). Symbol colors as in Figure 3. The average Pacific MORB plotted is the average of EPR data as compiled by Gale et al. (2013). EM = enriched mantle; FOZO = focus zone; DM = depleted mantle.

2008). In summary the volcanic stratigraphy of Savai'i supports our model of Samoan shield volcano geochemical evolution—with EM2 lavas at greatest depth, HIMU lavas at shallower levels, and an EM1 rejuvenated cap—with the caveat that there is no published data for a significant portion of the Savai'i shield stage (including the entire late shield stage).

Like Savai'i, the rejuvenated lavas of Upolu have Samoan EM1 isotopic compositions. However, in contrast to Savai'i, only ~50% of Upolu has been resurfaced with rejuvenated lavas (Konter & Jackson, 2012; Natland, 1980; Natland & Turner, 1985). Therefore, on Upolu the latest shield stage lavas are well exposed for sampling, and they display near-ubiquitous Samoan DM isotopic signatures (Jackson et al., 2014; Natland & Turner, 1985; Workman et al., 2004; Wright & White, 1987). A single lava of Samoan FOZO taxonomy has also been found on Upolu (Sample U39F; Workman et al., 2004; Jackson et al., 2014). This coeval eruption of lavas with Samoan FOZO and Samoan DM isotopic compositions is also observed in the upper shield lavas of the Tutuila drill core. Unfortunately, the submarine flanks of Upolu remain unsampled, so we cannot test whether the deepest volcanic stratigraphy at Upolu has erupted shield stage EM2 lavas. However, the exposed subaerial volcanic stratigraphy suggests that the latest shield and rejuvenated lavas of Upolu are consistent with the Tutuila drill core model for the isotopic evolution of a Samoan shield volcano, but



this comes with the caveat that the majority (>80%) of the volcanic stratigraphy of Upolu remains unsampled, because no submarine samples have been collected.

The remaining geochemically characterized volcanoes of the Samoan hotspot (e.g., Ofu, Ta'u, and Tupito [previously Muli], Malumalu, and Vailulu'u) lie to the east of Tutuila and appear to have a different geochemical evolution than the western volcanoes (Tutuila, Upolu, and Savai'i). We do not include Uo Mamae in this analysis because it does not clearly relate to volcanism produced by the Samoan hotspot. The eastern volcanoes have been divided into two en echelon lineaments, the Vai trend and Malu trend (Figure 1), based on their dominant isotopic compositions (dilute HIMU and EM2, respectively; Jackson et al., 2014; Koppers et al., 2011; Workman et al., 2004). Notably, the Malu and Vai trend volcanoes erupted contemporaneously (Koppers et al., 2011; Sims et al., 2008). Therefore, the dominant isotopic compositions of each lineament have been attributed to the Samoan mantle plume conveying different "plums" of material simultaneously erupting at geographically separate volcanic lineaments (Jackson et al., 2014; Koppers et al., 2011) indicating that, in addition to temporal geochemical evolution, there is also a geographic component to the geochemical variability in the eastern portion of the Samoan hotspot track. The two geochemically distinct volcanic trends in the eastern volcanoes may represent a "splitting" of the Samoan mantle plume into two separate eruptive lineaments sampling geochemically distinct plums. All volcanoes westward of, and including, Tutuila may sample similar plums of mantle material along a single trend, resulting in shield stage lavas that sample both FOZO (and in the case of Savai'i HIMU) and EM2 material. While the dominant isotopic compositions of the Malu and Vai volcanic lineaments are distinct, there is some geochemical overlap between the volcanoes of the two lineaments (i.e., some EM2 lavas are found in the HIMU lineament [Vai trend], and vice versa; see Figure S4). A similar splitting of a hotspot into two eruptive lineaments has been observed at Hawai'i, with the Loa and Kea lineaments splitting eastward of Oahu (Abouchami et al., 2005; Tanaka et al., 2008; Weis et al., 2011), a phenomenon that was posited by Jones et al. (2017) to be the result of a change in plate motion. Like the Samoan hotspot, a slight geochemical overlap between volcanoes from the two geographic lineaments has also been observed in Hawai'i (Abouchami et al., 2005; Harrison et al., 2017).

No EM1 rejuvenated stage lavas have been observed on the of the eastern volcanoes of the Samoan hotspot, because these eastern Samoan volcanoes—with the exception of sparsely sampled Malutut (1.04–1.48 Ma)—are younger than 1 Ma (Koppers et al., 2008, 2011; McDougall, 2010; Sims et al., 2008) and also have not yet passed over the flexural bulge. Similarly, no Samoan DM component has been observed on these volcanoes, which might be expected if the DM component is only erupted during the latter period of the shield stage of a Samoan volcano: only the western, older Samoan volcanoes, Upolu and Tutuila (and possibly the unsampled submarine portion of the late shield stage at Savai'i), exhibit the DM component. Geochronology suggests that the eastern Samoan volcanoes are still in the "early" to "middle" shield stage of their evolution, which may be too early in their volcanic evolution to capture the DM component.

While this drill core represents the most complete continuous section of Samoan volcanic stratigraphy, we cannot rule out further isotopic variability in the several kilometers of unsampled volcanic stratigraphy in the deepest shield stages at Tutuila. However, we do note that a lava from the only submarine dredge of Tutuila (ALIA-DR112), obtained at ~2,330 mbsl, has a clear EM2 signature that is consistent with EM2-type lavas found in the deepest portions of the Tutuila drill core. Nonetheless, the rejuvenated lavas at Tutuila provide critical insight into the timing of the onset of rejuvenated volcanism, which has not been well described on the other two Samoan Islands (Savai'i and Upolu) that exhibit rejuvenated volcanism. Below we explore the implications for constraining the timing of the onset of rejuvenated volcanism at Tutuila.

## 5.2. Tectonic Influence on Rejuvenated Volcanism

Two aspects of rejuvenated volcanism in Samoa distinguish it from rejuvenated volcanism at other hotspot: (1) the large volumes of Samoan rejuvenated volcanism and (2) the EM1-type geochemistry of the Samoan rejuvenated lavas. The Hawai'ian volcanoes have volumes of rejuvenated volcanism that are at most 0.1% of the total volcano volume (for Kauai; Garcia et al., 2010) and generally only cover a small extent of the sub-aerially exposed volcano (<6%) at the other Hawai'ian volcanoes (Clague & Sherrod, 2014; Garcia et al., 2010), except for Ni'ihau (Cousens & Clague, 2015). However, in Samoa, rejuvenated volcanism is much more voluminous, up to ~1.8% of the total volcano volume (estimated for Savai'i; Konter & Jackson, 2012)

and the coverage of rejuvenated volcanism ranges from near-complete coverage (99%) on Savai'i to ~15% on Tutuila (Konter & Jackson, 2012; Natland, 1980).

The origin of this anomalously voluminous rejuvenated volcanism (relative to volcano volume) is thought to be related to the proximity of the Samoan hotspot track to the northern terminus of the Tonga Trench, which induces tectonic stresses in the Samoan region that may enhance melting (Konter & Jackson, 2012; Koppers et al., 2008; Natland, 1980; Natland & Turner, 1985; Wright & White, 1987). Konter and Jackson (2012) hypothesized that the voluminous rejuvenated volcanism in Samoa is the result of decompression melting due to plate flexure as the Pacific plate is subducted at the Tonga Trench. Because tectonic stresses relating to the trench will vary as a function of distance from the trench (Hawkins & Natland, 1975; Natland, 1980), one prediction of this hypothesis (Hart et al., 2004; Koppers et al., 2008; Konter & Jackson, 2012) is that the timing of the onset of rejuvenated volcanism at a Samoan volcano should relate to the volcano's position with respect to the trench: as Samoan volcanoes are rafted westward toward the trench, tectonically induced rejuvenated volcanism will appear first in the western Samoan Islands (like Savai'i) before they appear in the eastern Samoan Islands (like Tutuila). The Tutuila drill core provides the first opportunity to test the hypothesis of a tectonic origin for Samoan rejuvenated volcanism because the geochronologic data from the Tutuila drill core capture the onset of rejuvenated volcanism at  $24.3 \pm 2.1$  ka, which places Tutuila ~150 km east of the trench axis at the onset of rejuvenated volcanism (Figure 10).

Govers and Wortel (2005) use a finite difference method to evaluate plate flexure as a tectonic plate tears and is partially subducted. Konter and Jackson (2012) apply the generalized plate flexure model of Govers and Wortel (2005) to the region encompassing Samoa and northern Tonga as a model for the "vertical velocity" of the Pacific plate resulting from plate flexure as the Pacific plate subducts into the Tonga Trench. We emphasize that this is a general model that is not specific to Samoa, but it does provide a framework for understanding plate flexure in the region near a slab tear. In Figure 10, the shaded orange area highlights the region where vertical velocities exceed 0.4 mm/year, which is the vertical velocity experienced by Tutuila at the onset of rejuvenated volcanism at 24.3 ka. At this time, Tutuila was ~150 km east of the trench (and Tutuila has moved only ~2 km further to the east during the past 24.3 ka).

If this vertical velocity contour reflects a threshold at which significant rejuvenated volcanism can be released from (or generated within; see Konter & Jackson, 2012) the melt zone at the base of the plate beneath other Samoan volcanoes, then this model can be used to predict the timing of the onset, and relative volumes, of rejuvenated volcanism at other, older Samoan volcanoes, including Upolu and Savai'i, located to the west of Tutuila. It is also possible that rejuvenated volcanism operates continuously at a Samoan volcano while it passes through the region of the Pacific plate with high ( $>0.4$  mm/year) vertical velocity (which is the orange shaded region between the two dashed lines in the panels of Figure 10). Note that in this simple model, we assume that the melt produced is erupted and does not account for melt segregation or transport.

This model is qualitatively consistent with the timing and relative volumes of rejuvenated volcanism on Savai'i. Savai'i lies within the region with  $>0.4$  mm/year vertical velocity and has had recent historical rejuvenated eruptions reported from 1905 to 1911 (Anderson, 1910; Sapper, 1906a). Going further back in time, the oldest dated Savai'i rejuvenated lava (0.39 Ma; Workman et al., 2004) also erupted when Savai'i was located within the region of high vertical velocity (see "0.39 Ma" panel in Figure 10). Unfortunately, no published data have captured the onset of rejuvenated volcanism at Savai'i, but rejuvenated lavas older than 0.39 Ma may exist. If Savai'i rejuvenated volcanism initiated when the lithosphere beneath the island achieved a vertical velocity of  $>0.4$  mm/year, then Savai'i rejuvenated volcanism is predicted to have initiated at ~1 Ma when Savai'i crossed into the region characterized by a vertical velocity  $> 0.4$  mm/year (see "1 Ma" panel in Figure 10). At this time, Savai'i would have been located approximately the same distance from the trench as Tutuila was at 24 ka.

Unfortunately, ages for lavas specifically mapped as rejuvenated lavas are not available on Upolu. Studies examining the ages of lavas on Upolu have specifically targeted shield lavas (McDougall, 2010; Natland & Turner, 1985; Workman et al., 2004). The youngest weighted  $^{40}\text{Ar}/^{39}\text{Ar}$  weighted plateau age for an Upolu lava is 0.933 Ma, and this lava is classified as shield stage based on field relationships and its radiogenic isotopic composition (Workman et al., 2004). The tectonic model predicts that rejuvenated volcanism would have initiated at ~0.6 Ma on Upolu. Kear and Wood (1959) and McDougall (2010) suggest that the rejuvenated volcanism on Upolu is  $<0.2$  Ma based on field observations, but this has not been confirmed with



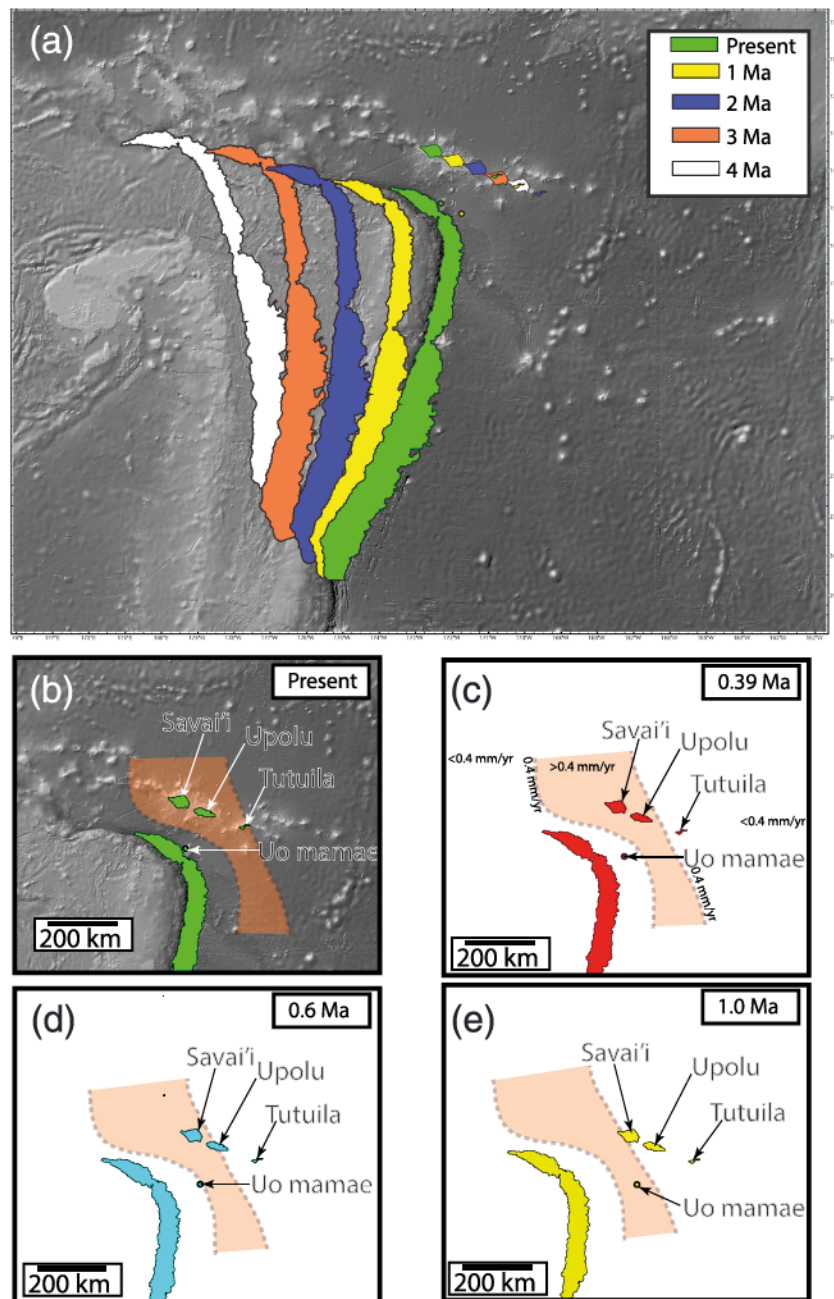


**Figure 10.** A map showing the tectonic evolution of the Samoan hotspot region over the last 4 Ma (panel a). Panels (b)–(e) show time steps at present (at 0.39, 0.6, and 1.0 Ma). The plate reconstruction is based on the method of Ruellan et al. (2003) and Hart et al. (2004), and the time evolution of the relative positions of the trench and the Samoan Islands is graphically illustrated in Koppers et al. (2008). The orange shaded region shows the region where upward plate velocity is  $>0.4$  mm/year, which corresponds to the onset of rejuvenated volcanism at Tutuila. This vertical velocity field is taken from the finite difference model of Govers and Wortel (2005), which was superimposed on the Samoa region by Konter and Jackson (2012). We here assume that the vertical velocity field from Govers and Wortel (2005) can be mapped onto the region back in time and assume that the position of the field is fixed with respect to the position of the trench (i.e., as the position of the trench moves east, so does the velocity field).

geochronology. Clearly, it will be important to sample the transition from shield to rejuvenated volcanism at Savai'i and Upolu to evaluate the hypothesis for the timing of the onset of Samoan rejuvenated volcanism proposed here.

It is worth noting that Savai'i has been situated atop the flexural bulge longer than Upolu or Tutuila (Figure 10), so it is expected to have the most rejuvenated melt, which is observed. Tutuila has only just reached the flexural bulge, so it is expected to have the least rejuvenated melt of the three islands, which is also observed.

There is another example of young volcanism in the Samoan region that may be related to the tectonic trigger proposed here. Located ~90 km south of Savai'i, a phonolite lava from Uo Mamae seamount was dated to 0.94 Ma (Hawkins & Natland, 1975). At the time this lava was erupted, Uo Mamae was within the region defined by >0.4-mm/year vertical velocity (Figure 10 shows that Uo Mamae was within the region of high vertical velocity between 0.6 and 1.0 Ma). This model, if accurate, suggests that volcanism may be widespread among submarine volcanoes, both Samoan and non-Samoan, in the zone of high vertical velocity outboard of the Tonga Trench.

Volcanism associated with flexure of oceanic lithosphere outboard of trenches is not limited to the Samoan hotspot. Recent work has revealed small, young seamounts called petit spots located outboard of several trenches globally, including the Japan Trench (Hirano et al., 2006; Machida et al., 2015), the Tonga Trench (Hirano et al., 2008), and the Chile Trench (Hirano et al., 2013). Petit spot volcanoes are proposed to be the result of volcanism associated with flexure of the oceanic lithosphere prior to subduction (Hirano et al., 2006). In this vein, young volcanism (here referred to as rejuvenated volcanism, owing to the protracted period of quiescence between its appearance and the earlier shield stage volcanism) is also reported on Christmas Island, located outboard of the Sunda Trench. Hoernle et al. (2011) and Taneja et al. (2015) inferred that the rejuvenated volcanism at Christmas Island is a result of tectonic stresses associated with the volcano's approach to the Sunda Trench, and Hoernle et al. (2011) even suggest that a mechanism similar to that generating volcanism at petit spots has also operated to generate rejuvenated volcanism on Christmas Island. The similarity between Samoan rejuvenated lavas to volcanic products related to plate flexure at other localities—including petit spot volcanoes and rejuvenated lavas at Christmas Island—is not limited to a common tectonic setting. We show below that lavas that have been characterized at petit spots also have geochemical similarities to Samoan rejuvenated lavas.

### 5.3. Geochemical Connection to Petit Spots

Rejuvenated lavas from other hotspots located far from trenches—like Hawai'i (Cousens & Clague, 2015; Dixon et al., 2008; Garcia et al., 2010; Weis et al., 2011), the Societies (White & Duncan, 1996), Madeira (Geldmacher & Hoernle, 2000), Mauritius (Paul et al., 2005), and the Canary Islands (Hoernle et al., 1991; Geldmacher et al., 2005)—commonly exhibit radiogenic isotopic compositions that are geochemically depleted relative to the shield stage. However, other hotspots have rejuvenated lavas that are more enriched than their shield stage. One case is Kerguelen, where there is significant evidence for continental material (Paul et al., 2005; Weis & Frey, 2002), so we cannot exclude the possibility of continental assimilation in the rejuvenated lavas. Another case is the Marquesas, where lithospheric processes (Woodhead, 1992), or different mantle sources (Legendre et al., 2005; Legendre et al., 2005), have been hypothesized to control the enrichment of the rejuvenated lavas relative to the shield lavas; at the Marquesas, the rejuvenated lavas are shifted toward the same EM2 mantle component as the Marquesas shield stage lavas. A unique case is that of the Tristan-Gough hotspot track, where the EM1 shield stage is veneered with HIMU composition rejuvenated lavas which have been hypothesized to be the result of either small HIMU blobs, or a second mantle plume rising from the core mantle boundary or HIMU material linked to Africa due to the presence of late-stage HIMU volcanism only on the portion of the hotspot track closest to the continental margin (Homrighausen et al., 2018).

In Samoa, rejuvenated lavas are more geochemically enriched than much (but not all) of the shield stage (Jackson et al., 2014; Konter & Jackson, 2012; Wright & White, 1987), but the rejuvenated lavas are shifted toward an EM1 component like that sampled at nearby Uo Mamae seamount (Figures 1 and 9). An EM1 component is not sampled by Samoan shield stage lavas. We note that the EM1 component is highly heterogeneous but exhibits broad geochemical similarities—low  $^{143}\text{Nd}/^{144}\text{Nd}$  at a given  $^{87}\text{Sr}/^{86}\text{Sr}$  and high  $^{208}\text{Pb}/^{204}\text{Pb}$  at a given  $^{206}\text{Pb}/^{204}\text{Pb}$ —globally. With this in mind, rejuvenated lavas at Christmas Island, and petit spot lavas outboard of the Japan Trench, host clear but geochemically heterogeneous EM1 components. Ba enrichment, a feature noted to be common to EM1 lavas (Hart et al., 2004), is shared by rejuvenated lavas at Christmas Island, petit spot lavas outboard of the Japan Trench, Uo Mamae, and the Samoan rejuvenated



lavas (Figure S3). Unlike the other hotspots that exhibit rejuvenated volcanism, the Samoan volcanoes are situated near a subduction zone where, like Christmas Island and petit spots near the Japan Trench, a tectonic mechanism may trigger release of rejuvenated lavas with EM1 compositions. Below we discuss a possible association between EM1 signatures and oceanic volcanism that is triggered by tectonic stresses in the outer rise of subduction zone settings.

Recent Sr-Nd-Hf-Pb isotopic analyses of petit spot volcanoes outboard of the Japan Trench reveal that they also host EM1 isotopic compositions (Machida et al., 2009, 2015). The discovery of extreme EM1 lavas in petit spots was unexpected, given their location far from known mantle plumes (Machida et al., 2009). The lack of known hotspot tracks in the region of the Japanese petit spots rules out an EM1 contribution from a mantle plume. Similarly, the young volcanism observed on Christmas Island, hypothesized to be the result of “petit spot-like” lithospheric flexure as the island approaches the Sunda Trench (Hoernle et al., 2011; Taneja et al., 2015), also has clear EM1 isotopic signatures. Therefore, we suggest a common EM1 signature in petit spot volcanoes at these localities. This model would suggest a shallow mantle source for the EM1 signature, given the lack of observed deep-seated mantle plumes at these petit spot volcanoes. However, a shallow mantle source for the EM1 endmember at petit spots and petit spot volcanoes is not wholly unexpected: previously published work also suggested a shallow origin for EM1 signatures identified at several other intraplate volcanic settings (Class & le Roex, 2011; Geldmacher et al., 2008; Gibson et al., 2005; Konter & Becker, 2012; Regelous et al., 2009). The examples of petit spot volcanoes outboard of the Japanese Trench and volcanism at Christmas Island require a nonplume-related source for EM1 isotopic signatures, and this would fit the example of rejuvenated volcanism at Samoa, suggesting that tectonic processes operating in the lithosphere can tap reservoirs with EM1 signatures that exist in the shallowest upper mantle. Konter and Jackson (2012) attribute the EM1 signatures in rejuvenated Samoan lavas to these lavas sampling Samoan lithosphere previously metasomatized by the Rarotonga plume. Metasomatism of the oceanic lithosphere by a mantle plume sampling an EM1 reservoir may explain the EM1 rejuvenated lavas in Samoa but cannot explain the EM1 isotopic signatures of the Japanese petit spot lavas or late stage Christmas Island lavas as no hotspot tracks are observed near the Japanese petit spots or Christmas Island. Nonetheless, the EM1 signature in Samoan rejuvenated lavas is not tapped during the shield-building stage, suggesting that this component is not hosted in the Samoan plume, but melts generated by tectonic stresses associated with approach to the trench tap the EM1 signature, consistent with an upper mantle residence.

Jackson et al. (2018) observed that EM isotopic signatures are less correlated with putative mantle plumes than other mantle endmembers like HIMU, presenting the possibility that EM signatures could be the result of melting deep and shallow mantle reservoirs. New observations of EM1 volcanism unrelated to mantle plumes at rejuvenated Christmas Island (Hoernle et al., 2011), rejuvenated Samoan lavas, and nonplume-related Japanese petit spot lavas support the hypothesis that EM1 isotopic signatures are not solely related to a deep mantle enriched reservoir but can instead be sourced from the shallow upper mantle. However, it is not clear how a widespread enriched mantle reservoir can exist in the shallow oceanic asthenosphere which has previously been depleted by high degrees of melting at mid-ocean ridges: The oceanic lithosphere beneath Japanese petit spots, Samoa, and Christmas Island is Cretaceous in age. An important question, therefore, is how the EM1 signature came to reside in the shallow mantle at these localities following depletion of the shallow mantle by melt extraction at Cretaceous mid-ocean ridges. It is possible that this depleted material may be wholly or partially replaced over geologic time as the lithosphere moves away from the ridge. As oceanic lithosphere ages and cools, small-scale sublithospheric convection may develop that is driven by thermal boundary layer instabilities (Ballmer et al., 2007, 2010; Huang et al., 2003). Importantly, Ballmer et al.'s (2007, 2011) models indicate that during small-scale sublithospheric convection, DM downwells and is replaced with fertile peridotite that rises from greater depths. If small-scale sublithospheric convection is occurring under wide swaths of ancient oceanic lithosphere, like the Cretaceous lithosphere upon which the petit spot volcanoes (including rejuvenated lavas at Samoan and Christmas Islands) are constructed, then such shallow convection could transport enriched mantle material—possibly as fertile plums—from deeper within the mantle into the otherwise depleted shallow mantle. This newly supplied fertile peridotite could be the shallow EM1 reservoir that is tapped by petit spots, including rejuvenated volcanism at Christmas Island and Samoan rejuvenated volcanism (including Uo Mamae). One hypothesis for the origin of EM1 signatures in the shallow mantle is the presence of stranded subcontinental lithospheric mantle or the lower crust that remained in the upper mantle (e.g., Hoernle et al., 2011; Konter &

Becker, 2012). However, Samoa's location in the southwest Pacific is not clearly related to the locus of known continental rifting, so linking Samoan EM1 volcanism with continental materials stranded in the upper mantle is challenging. Therefore, the origin of the EM1 signature sampled by petit spot lavas, and how it came to be in the shallow mantle, remains an important outstanding problem.

## Acknowledgments

Reviews from Kaj Hoernle and three anonymous reviewers are gratefully acknowledged. M. G. J. acknowledges support from the American Samoa Power Authority and National Science Foundation grants OCE-1736984 and EAR-1624840. The Tutuila drill core was the brainchild of Tim Bodell, without whom we would still have no stratigraphic record of Tutuila volcanism. The support of Utu Abe Malae and Matamua Katrina Mariner was instrumental to the project's success. We dedicate this paper to the memory of Abe Malae and his efforts to support science and education in American Samoa. Images of the entire drill core are available online ([escholarship.org/uc/item/6gg6p61w](https://escholarship.org/uc/item/6gg6p61w)). All data presented are either part of this study or previously published and are referenced in text.

## References

- Abouchami, W. H., Hofmann, A. W., Galer, S. J. G., Frey, F. A., Eisel, J., & Feigenson, M. (2005). Lead isotopes reveal bilateral asymmetry and vertical continuity in the Hawaiian mantle plume. *Nature*, 434(7035), 851–856. <https://doi.org/10.1038/nature03402>
- Anderson, T. (1910). The volcano of Matavanu in Savaii. *Quarterly Journal of the Geological Society London*, 66(1-4), 621–639. <https://doi.org/10.1144/GSLJGS.1910.066.01-04.30>
- Ballmer, M. D., Ito, G., van Hunen, J., & Tackley, P. J. (2010). Small-scale sublithospheric convection reconciles geochemistry and geochronology of 'Superplume' volcanism in the western and south Pacific. *Earth and Planetary Science Letters*, 290(1-2), 224–232. <https://doi.org/10.1016/j.epsl.2009.12.025>
- Ballmer, M. D., Ito, G., van Hunen, J., & Tackley, P. J. (2011). Spatial and temporal variability in Hawaiian hotspot volcanism induced by small-scale convection. *Nature Geoscience*, 4(7), 457–460. <https://doi.org/10.1038/ngeo1187>
- Ballmer, M. D., van Hunen, J., Ito, G., Tackley, P. J., & Bianco, T. A. (2007). Non-hotspot volcano chains originating from small-scale sublithospheric convection. *Geophysical Research Letters*, 34, L23310. <https://doi.org/10.1029/2007GL031636>
- Bard, E., Hamelin, B., Arnold, M., Montaggioni, L., Cabioch, G., Faure, G., & Rougerie, F. (1996). Deglacial sea level record from Tahiti corals and the timing of global meltwater discharge. *Nature*, 382(6588), 241–244. <https://doi.org/10.1038/382241a0>
- Bevis, M., Taylor, F. W., Schutz, B. E., Recy, J., Isacks, B. L., Helu, S., et al. (1995). Geodetic observations of very rapid convergence and back-arc extension at the Tonga arc. *Nature*, 374(6519), 249–251. <https://doi.org/10.1038/374249a0>
- Bianco, T. A., Ito, G., Becker, J. M., & Garcia, M. O. (2005). Secondary Hawaiian volcanism formed by flexural arch decompression. *Geochemistry, Geophysics, Geosystems*, 6, Q08009. <https://doi.org/10.1029/2005GC000945>
- Caroff, M., Guillou, H., Lamiaux, M. L., Maury, R. C., Guille, G., & Cotton, J. (1999). Assimilation of ocean crust by hawaiitic and mugearitic magmas: An example from Eiao (Marquesas). *Lithos*, 46(2), 235–258. [https://doi.org/10.1016/S0024-4937\(98\)00068-1](https://doi.org/10.1016/S0024-4937(98)00068-1)
- Chang, S.-J., Ferreira, A. M. G., & Faccenda, M. (2016). Upper- and mid-mantle interaction between the Samoan plume and the Tonga-Kermadec slabs. *Nature Communications*, 7(1), 10799. <https://doi.org/10.1038/ncomms10799>
- Clague, D. A., & Sherrod, D. R. (2014). The growth and degradation of Hawaiian volcanoes. US Geol. Surv. Prof. Paper 1801
- Class, C., & le Roex, A. (2011). South Atlantic DUPAL anomaly—Dynamic and compositional evidence against a recent shallow origin. *Earth and Planetary Science Letters*, 305(1-2), 92–102. <https://doi.org/10.1016/j.epsl.2011.02.036>
- Cousens, B. L., & Clague, D. A. (2015). Shield to rejuvenated stage volcanism on Kauai and Niihau, Hawaiian Islands. *Journal of Petrology*, 56(8), 1547–1584. <https://doi.org/10.1093/ptrology/egv045>
- Dixon, J., Clague, D. A., Cousens, B., Monsalve, M. L., & Uhl, J. (2008). Carbonatite and silicate melt metasomatism of the mantle surrounding the Hawaiian plume: Evidence from volatiles, trace elements, and radiogenic isotopes in rejuvenated-stage lavas from Niihau, Hawaii. *Geochemistry, Geophysics, Geosystems*, 9, Q09005. <https://doi.org/10.1029/2008GC002076>
- Eisele, J., Abouchami, W., Galer, S. J., & Hofmann, A. W. (2003). The 320 kyr Pb isotope evolution of Mauna Kea lavas recorded in the HSDP 2 drill core. *Geochemistry, Geophysics, Geosystems*, 4(5), 8710. <https://doi.org/10.1029/2002GC000339>
- Falloon, T. J., Danyushevsky, L. V., Crawford, A. J., Maas, R., Woodhead, J. D., Eggins, S. M., et al. (2007). Multiple mantle plume components involved in the petrogenesis of subduction related lavas from the northern termination of the Tonga Arc and northern Lau Basin: Evidence from the geochemistry of arc and backarc submarine volcanics. *Geochemistry, Geophysics, Geosystems*, 2007, 8, Q09003. <https://doi.org/10.1029/2007GC001619>
- Farley, K. A., Natland, J. H., & Craig, H. (1992). Binary mixing of enriched and undegassed (primitive?) mantle components (He, Sr, Nd, Pb) in Samoan lavas. *Earth and Planetary Science Letters*, 111(1), 183–199. [https://doi.org/10.1016/0012-821X\(92\)90178-X](https://doi.org/10.1016/0012-821X(92)90178-X)
- Flower, M., Pritchard, R., Brem, G., Cann, J., Delaney, J., Emmerman, R., et al. (1982). Chemical stratigraphy, Iceland Research Drilling Project, Reydarfjörður, eastern Iceland. *Journal of Geophysical Research*, 87(B8), 6489–6510. <https://doi.org/10.1029/JB087iB08p06489>
- French, S. W., & Romanowicz, B. (2015). Broad plumes rooted at the base of the Earth's mantle beneath major hotspots. *Nature*, 525(7567), 95–99. <https://doi.org/10.1038/nature14876>
- Gale, A., Dalton, C. A., Langmuir, C. H., Su, Y., & Schilling, J. G. (2013). The mean composition of ocean ridge basalts. *Geochemistry, Geophysics, Geosystems*, 14, 489–518.
- Garcia, M. O., Haskins, E. H., Stolper, E. M., & Baker, M. (2007). Stratigraphy of the Hawai'i Scientific Drilling Project core (HSDP2): Anatomy of a Hawaiian shield volcano. *Geochemistry, Geophysics, Geosystems*, 8, Q02G20. <https://doi.org/10.1029/2006GC001379>
- Garcia, M. O., Swinnard, L., Weis, D., Greene, A. R., Tagami, T., Sano, H., & Gandy, C. E. (2010). Petrology, geochemistry and geochronology of Kaua'i lavas over 4.5 Myr: Implications for the origin of rejuvenated volcanism and the evolution of the Hawaiian plume. *Journal of Petrology*, 51, 1507–1540.
- Garcia, M. O., Weis, D., Jicha, B. R., Ito, G., & Hanano, D. (2016). Petrology and geochronology of lavas from Kaula Volcano: Implications for rejuvenated volcanism of the Hawaiian mantle plume. *Geochimica et Cosmochimica Acta*, 185, 278–301. <https://doi.org/10.1016/j.gca.2016.03.025>
- Geldmacher, J., & Hoernle, K. (2000). The 72 Ma geochemical evolution of the Madeira hotspot (eastern North Atlantic): Recycling of Paleozoic (<500 Ma) basaltic and gabbroic crust. *Earth and Planetary Science Letters*, 183(1-2), 73–92 (Corrigendum in Geldmacher, J., Hoernle, K., 2001. *Earth Planet. Sci. Lett.* 186, 333. [https://doi.org/10.1016/S0012-821X\(00\)00266-1](https://doi.org/10.1016/S0012-821X(00)00266-1)
- Geldmacher, J., Hoernle, K., Bogaard, P. V. D., Duggen, S., & Werner, R. (2005). New 40Ar/39Ar age and geochemical data from seamounts in the Canary and Madeira volcanic province: Support for the mantle plume hypothesis. *Earth and Planetary Science Letters*, 237(1-2), 85–101. <https://doi.org/10.1016/j.epsl.2005.04.037>
- Geldmacher, J., Hoernle, K., Klugel, A., van den Bogaard, P., & Bindeman, I. (2008). Geochemistry of a new enriched mantle type locality in the northern hemisphere: Implications for the origin of the EM1 source. *Earth and Planetary Science Letters*, 265(1-2), 167–182. <https://doi.org/10.1016/j.epsl.2007.10.001>
- Gibson, S., Thompson, R., Day, J., Humphris, S., & Dickin, A. (2005). Melt-generation processes associated with the Tristan mantle plume: Constraints on the origin of EM-1. *Earth and Planetary Science Letters*, 237, 744–767. <https://doi.org/10.1016/j.epsl.2005.06.015>



- Glover, E. A., & Taylor, J. D. (2001). Systematic revision of Australian and Indo-Pacific Lucinidae (Mollusca: Bivalvia): Pillucina, Wallucina and descriptions of two new genera and four new species. *Records of the Australian Museum*, 53(3), 263–292. <https://doi.org/10.3853/j.0067-1975.53.2001.1349>
- Govers, R., & Wortel, M. J. R. (2005). Lithosphere tearing at STEP faults: Response to edges of subduction zones. *Earth and Planetary Science Letters*, 236(1–2), 505–523. <https://doi.org/10.1016/j.epsl.2005.03.022>
- Hamelin, C., Dosso, L., Hanan, B., Moreira, M., Kositsky, A. P., & Thomas, M. Y. (2011). Geochemical portray of the Pacific ridge: New isotopic data and statistical techniques. *Earth and Planetary Science Letters*, 302(1–2), 154–162. <https://doi.org/10.1016/j.epsl.2010.12.007>
- Hanan, B., & Graham, D. (1996). Lead and helium isotope evidence from oceanic basalts for a common deep source of mantle plumes. *Science*, 272, 991–995. <https://doi.org/10.1126/science.272.5264.991>
- Harrison, L. N., Weis, D., & Garcia, M. O. (2017). The link between Hawaiian mantle plume composition, magmatic flux, and deep mantle geodynamics. *Earth Planetary Science Letters*, 463, 298–309. <https://doi.org/10.1016/j.epsl.2017.01.027>
- Hart, S. R., & Blusztajn, J. (2006). Age and geochemistry of the mafic sills, ODP site 1276, New Foundland margin. *Chemical Geology*, 235, 222–237. <https://doi.org/10.1016/j.chemgeo.2006.07.001>
- Hart, S. R., Coetzee, M., Workmana, R. K., Blusztajn, J., Sinton, J. M., Steinberger, B., & Hawkins, J. W. (2004). Genesis of the Western Samoa seamount province: Geochemical fingerprint and tectonics. *Earth and Planetary Science Letters*, 227(1–2), 37–56. <https://doi.org/10.1016/j.epsl.2004.08.005>
- Hart, S. R., Hauri, E., Oschmann, L., & Whitehead, J. (1992). Mantle plumes and entrainment: Isotopic evidence. *Science*, 256, 517–520. <https://doi.org/10.1126/science.256.5056.517>
- Hart, S. R., & Jackson, M. G. (2014). Ta'u and Ofu/Olosega volcanoes: The “twin sisters” of Samoa, their P, T, X melting regime, and global implications. *Geochemistry, Geophysics, Geosystems*, 15, 2301–2318. <https://doi.org/10.1002/2013GC005221>
- Hart, S. R., Staudigel, H., Koppers, A. A. P., Blusztajn, J., Baker, E. T., Workman, R., et al. (2000). Vailulu'u undersea volcano: The New Samoa. *Geochemistry, Geophysics, Geosystems*, 1, Paper number 2000GC000108 Published December 8, 2000(12). <https://doi.org/10.1029/2000GC000108>
- Hawkins, J. W., & Natland, J. H. (1975). Nephelinites and basanites of the Samoan linear volcanic chain: Their possible tectonic significance. *Earth and Planetary Science Letters*, 24(3), 427–439. [https://doi.org/10.1016/0012-821X\(75\)90150-8](https://doi.org/10.1016/0012-821X(75)90150-8)
- Hirano, N., Kawamura, K., Hattori, M., Saito, K., & Ogawa, Y. (2001). A new type of intra-plate volcanism: young alkali basalts discovered from the subducting Pa-cific Plate, northern Japan Trench. *Geophysical Research Letters*, 28(14), 2719–2722. <https://doi.org/10.1029/2000GL012426>
- Hirano, N., Koppers, A. A. P., Takahashi, A., Fujiwara, T., & Nakanishi, M. (2008). Seamounts, knolls and petit spot monogenetic volcanoes on the subducting Pacific Plate. *Basin Research*, 20(4), 543–553. <https://doi.org/10.1111/j.1365-2117.2008.00363.x>
- Hirano, N., Machida, S., Abe, N., Morishita, T., Tamura, A., & Arai, S. (2013). Petit-spot lava fields off the central Chile trench induced by plate flexure. *Geochemical Journal*, 47(2), 249–257. <https://doi.org/10.2343/geochemj.2.0227>
- Hirano, N., Takahashi, E., Yamamoto, J., Abe, N., Ingle, S. P., Kaneoka, I., et al. (2006). Volcanism in response to plate flexure. *Science*, 313(5792), 1426–1428. <https://doi.org/10.1126/science.1128235>
- Hoernle, K., Hauff, F., Werner, R., van den Bogaard, P., Gibbons, A. D., Conrad, S., & Müller, R. D. (2011). Origin of Indian Ocean Seamount Province by shallow recycling of continental lithosphere. *Nature Geoscience*, 4, 883–887.
- Hoernle, K., Tilton, G., & Schmincke, H.-U. (1991). Sr–Nd–Pb isotopic evolution of Gran Canaria: Evidence for shallow enriched mantle beneath the Canary Islands. *Earth and Planetary Science Letters*, 106, 44–63.
- Homrighausen, S., Hoernle, K., Geldmacher, J., Wartho, J.-A., Hauff, F., Portnyagin, M., et al. (2018). Unexpected HIMU-typelate-stage volcanism on the Walvis Ridge. *Earth and Planetary Science Letters*, 492, 251–263. <https://doi.org/10.1016/j.epsl.2018.03.049>
- Huang, J. S., Zhong, S. J., & van Hunen, J. (2003). Controls on sublithospheric small-scale convection. *Journal of Geophysical Research*, 108(B8), 2405. <https://doi.org/10.1029/2003JB002456>
- Jackson, M. G., Becker, T. W., & Konter, J. G. (2018). Evidence for a deep mantle source for EM and HIMU domains from integrated geochemical and geophysical constraints. *Earth and Planetary Science Letters*, 484, 154–167. <https://doi.org/10.1016/j.epsl.2017.11.052>
- Jackson, M. G., & Hart, S. R. (2006). Strontium isotopes in melt inclusions from Samoan basalts: Implications for heterogeneity in the Samoan plume. *Earth and Planetary Science Letters*, 245(1–2), 260–277. <https://doi.org/10.1016/j.epsl.2006.02.040>
- Jackson, M. G., Hart, S. R., Konter, J. G., Kurz, M. D., Blusztajn, J., & Farley, K. A. (2014). Helium and lead isotopes reveal the geochemical geometry of the Samoan plume. *Nature*, 514, 355–358.
- Jackson, M. G., Hart, S. R., Konter, J. P., Koppers, A. A. P., Staudigel, H., Kurz, M. D., et al. (2010). The Samoan hotspot track on a “hotspot highway”: Implications for mantle plumes and a deep Samoan mantle source. *Geochemistry, Geophysics, Geosystems*, 11, Q12009. <https://doi.org/10.1029/2010GC003232>
- Jackson, M. G., Hart, S. R., Koppers, A. A. P., Staudigel, H., Konter, J., Blusztajn, J., et al. (2007). The return of subducted continental crust in Samoan lavas. *Nature*, 448, 684–687.
- Jochum, K. P., Weis, U., Schwager, B., Stoll, B., Wilson, S. A., Haug, G. H., et al. (2015). Reference values following ISO guidelines for frequently requested rock reference materials. *Geostandards and Geoanalytical Research*, 40(3), 333–350. <https://doi.org/10.1111/j.1751-908X.2015.00392.x>
- Johnson, D. M., Hooper, P. R., & Conrey, R. M. (1999). XRF Analysis of rocks and minerals for major and trace elements on a single low dilution Li-tetraborate fused bead. *Advances in X-Ray Analysis*, 41, 843–867.
- Jones, T. D., Davies, D. R., Campbell, I. H., Iaffaldano, G., Yaxley, G., Kramer, S. C., & Wilson, C. R. (2017). The concurrent emergence and causes of double volcanic hotspot tracks on the Pacific plate. *Nature*, 545(7655), 472.
- Kear, D., & Wood, B. L. (1959). The geology and hydrology of Western Samoa. *New Zealand Geological Survey Bulletin*, 63, 1–90.
- Knaack, C., Cornelius, S., & Hooper, P. (1994). Trace element analyses of rocks and minerals by ICP-MS. Open-File Report. Washington State University.
- Konrad, K., Koppers, A. A. P., Steinberger, B., Finlayson, V., Konter, J. G., & Jackson, M. G. (2018). On the relative motion of long-lived Pacific mantle plumes. *Nature Communications*, 9(1), 854. <https://doi.org/10.1038/s41467-018-03277-x>
- Konter, J. G., & Becker, T. W. (2012). Shallow lithospheric contribution to mantle plumes revealed by integrating seismic and geochemical data. *Geochemistry, Geophysics, Geosystems*, 13, Q02004. <https://doi.org/10.1029/2011GC003923>
- Konter, J. G., & Jackson, M. G. (2012). Large volumes of rejuvenated volcanism in Samoa: Evidence supporting a tectonic influence on late-stage volcanism. *Geochemistry, Geophysics, Geosystems*, 13, Q0AM04. <https://doi.org/10.1029/2011GC003974>
- Koppers, A. A. (2002). ArArCALC—software for <sup>40</sup>Ar/<sup>39</sup>Ar age calculations. *Computers & Geosciences*, 28(5), 605–619.
- Koppers, A. A. P., Russell, J. A., Jackson, M. G., Konter, J., Staudigel, H., & Hart, S. R. (2008). Samoa reinstated as a primary hotspot trail. *Geology*, 36, 435–438.

- Koppers, A. A. P., Russell, J. A., Roberts, J., Jackson, M. G., Konter, J. G., Wright, D. J., et al. (2011). Age systematics of two young en echelon Samoan volcanic trails. *Geochemistry, Geophysics, Geosystems*, 12, Q07025. <https://doi.org/10.1029/2010GC003438>
- Koppers, A. A. P., & Sager, W. W. (2014). Large-scale and long-term volcanism on oceanic lithosphere. *Developments in Marine Geology*, 7, 553–557. <https://doi.org/10.1016/B978-0-444-62617-2.00019-0>
- Koppers, A. A. P., Staudigal, H., Pringle, M. S., & Wijbrans, J. R. (2003). Short-lived and discontinuous intraplate volcanism in the South Pacific: Hot spots or extensional volcanism? *Geochemistry, Geophysics, Geosystems*, 4(10), 1089. <https://doi.org/10.1029/2003GC000533>
- Kuiper, K. F., Deino, A., Hilgen, F. J., Krijgsman, W., Renne, P. R., & Wijbrans, J. R. (2008). Synchronizing rock clocks of Earth history. *Science*, 320, 500–504. <https://doi.org/10.1126/science.1154339>
- Kurz, M. D., Kenna, T. C., Lassiter, J. C., & DePaolo, D. J. (1996). Helium isotopic evolution of Mauna Kea Volcano: First results from the 1-km drill core. *Journal of Geophysical Research*, 101, 11,781–11,791. <https://doi.org/10.1029/95JB03345>
- Lassiter, J. C., DePaolo, D. J., & Tatsumoto, M. (1996). Isotopic evolution of Mauna Kea volcano: Results from the initial phase of the Hawaiian Scientific Drilling Project. *Journal of Geophysical Research*, 101(B5), 11,769–11,780. <https://doi.org/10.1029/96JB00181>
- le Maitre, R. W. (2002). *Igneous rocks. A classification and glossary of terms. Recommendations of the international union of geological sciences subcommission on the systematics of igneous rocks* (2nd ed., p. 254). Cambridge, UK: Cambridge University Press.
- Legendre, C., Maury, R. C., Caroff, M., Guillou, H., Cotten, J., Chauvel, C., et al. (2005). Origin of exceptionally abundant phonolites on Ua Pou island (Marquesas, French Polynesia): Partial melting of basanites followed by crustal contamination. *Journal of Petrology*, 46(9), 1925–1962. <https://doi.org/10.1093/petrology/egi043>
- Legendre, C., Maury, R. C., Savanier, D., Cotten, J., Chauvel, C., Hémond, C., et al. (2005). The origin of intermediate and evolved lavas in the Marquesas archipelago: An example from Nuku Hiva island (French Polynesia). *Journal of Volcanology and Geothermal Research*, 143, 293–317. <https://doi.org/10.1016/j.jvolgeores.2004.12.001>
- Macdonald, G. A., & Katsura, T. (1964). Chemical composition of the Hawaiian lavas. *Journal of Petrology*, 5, 83–133.
- Machida, S., Hirano, N., & Kimura, J.-I. (2009). Evidence for recycled plate material in Pacific upper mantle unrelated to plumes. *Geochim. Cosmochim. Acta*, 73, 3028–3037. <https://doi.org/10.1016/j.gca.2009.01.026>
- Machida, S., Hirano, N., Sumino, H., Hirata, T., Yoneda, S., & Kato, Y. (2015). Petit-spot geology reveals melts in upper-most asthenosphere dragged by lithosphere. *Earth and Planetary Science Letters*, 426, 267–279. <https://doi.org/10.1016/j.epsl.2015.06.018>
- Maguire, R., Ritsema, J., & Goes, S. (2017). Signals of 660 km topography and harzburgite enrichment in seismic images of whole-mantle upwellings. *Geophysical Research Letters*, 44, 3600–3607. <https://doi.org/10.1002/2017GL073120>
- McDougall, I. (2010). Age of volcanism and its migration in the Samoa Islands. *Geological Magazine*, 147(5), 705–717. <https://doi.org/10.1017/S0016756810000038>
- Min, K. W., Mundil, R., Renne, P. R., & Ludwig, K. R. (2000). A test for systematic errors in Ar-40/Ar-39 geochronology through comparison with U/Pb analysis of a 1.1-Ga rhyolite. *Geochimica et Cosmochimica Acta*, 64(1), 73–98. [https://doi.org/10.1016/S0016-7037\(99\)00204-5](https://doi.org/10.1016/S0016-7037(99)00204-5)
- Natland, J. H. (1980). The progression of volcanism in the Samoan linear volcanic chain. *American Journal of Science*, 280A, 709–735.
- Natland, J. H., & Turner, D. L. (1985). In T. M. Brocher (Ed.), *Age progression and petrological development of Samoan shield volcanoes: Evidence from K-Ar ages, lava compositions, and mineral studies, Investigations of the Northern Melanesian Borderland, Earth Sci. Ser., vol. 3* (pp. 139–171). Houston, TX: Circum-Pacific Council for Energy and Mineral Resources.
- Neal, C. R., Mahoney, J. J., & Chazey, W. J. III (2002). Mantle sources and the highly variable role of continental lithosphere in basalt petrogenesis of the Kerguelen Plateau and Broken Ridge LIP: Results from ODP Leg 183. *Journal of Petrology*, 43(7), 1177–1205. <https://doi.org/10.1093/petrology/43.7.1177>
- Paul, D., White, W. M., & Blichert-Toft, J. (2005). Geochemistry of Mauritius and the origin of rejuvenescent volcanism on oceanic island volcanoes. *Geochemistry, Geophysics, Geosystems*, 6, Q06007. <https://doi.org/10.1029/2004GC000883>
- Phelan, M. (1999). A  $\Delta R$  correction value for Samoa from known-age marine shells. *Radiocarbon*, 41(01), 99–101. <https://doi.org/10.1017/S003822200019366>
- Regelous, M., Niu, Y. L., Abouchami, W., & Castillo, P. R. (2009). Shallow origin for South Atlantic Dupal Anomaly from lower continental crust: Geochemical evidence from the Mid-Atlantic Ridge at 26°S. *Lithos*, 112, 57–72. (this issue)
- Regelous, M., Turner, S., Falloon, T. J., Taylor, P., Gamble, J., & Green, T. (2008). Mantle dynamics and mantle melting beneath Niuafo'ou Island and the northern Lau back-arc basin. *Contributions to Mineralogy and Petrology*, 156(1), 103–118. <https://doi.org/10.1007/s00410-007-0276-7>
- Reimer, P. J., Bard, E., Bayliss, A., Beck, J. W., Blackwell, P. G., Ramsey, C. B., et al. (2013). INTCAL13 AND MARINE13 radiocarbon age calibration curves 0–50,000 years cal BP. *Radiocarbon*, 55(04), 1869–1887. [https://doi.org/10.2458/azu\\_js\\_rc.55.16947](https://doi.org/10.2458/azu_js_rc.55.16947)
- Ruellan, E., Delteil, J., Wright, I., & Matsumoto, T. (2003). From rifting to active spreading in the Lau Basin–Havre Trough backarc system (SW Pacific)—locking/unlocking induced by seamount chain subduction. *Geochemistry, Geophysics, Geosystems*, 4(5), 8909. <https://doi.org/10.1029/2001GC000261>
- Sapper, K. (1906a). Der Matavanu-Ausbruch auf Savai'i 1905/06. Nach Aufzeichnungen von Pater Mennel, Mitteilungen von Dr. B. Funk und gedruckten Berichten dargestellt. *Z. Gesellschaft Erdkunde Berlin*, 41, 686–709.
- Sims, K. W. W., Hart, S. R., Reagan, M. K., Blusztajn, J., Staudigal, H., Sohn, R. A., et al. (2008). 238U–230Th–226Ra–210Pb–210Po, 232Th–228Ra, and 235U–231Pa constraints on the ages and petrogenesis of Vailulu'u and Malumalu Lavas, Samoa. *Geochemistry, Geophysics, Geosystems*, 9, Q04003. <https://doi.org/10.1029/2007GC001651>
- Staudigal, H., Hart, S. R., Pile, A., Bailey, B. E., Baker, E. T., Brooke, S., et al. (2006). Vailulu'u Seamount, Samoa: Life and death on an active submarine volcano. *Proceedings of the National Academy of Sciences*, 103, 6448–6453. <https://doi.org/10.1073/pnas.0600830103>
- Stearns, H. T. (1944). Geology of the Samoan Islands. *GSA Bull.*, 55(11), 1279–1332. <https://doi.org/10.1130/GSAB-55-1279>
- Steiger, R. H., & Jäger, E. (1977). Subcommittee on geochronology: Convention on the use of decay constants in geo- and cosmochronology. *Earth and Planetary Science Letters*, 36(3), 359–362.
- Takamasa, A., & Nakai, S. (2009). Contamination introduced during rock sample powdering: Effects from different mill materials on trace element contamination. *Geochemical Journal*, 43(5), 389–394. <https://doi.org/10.2343/geochimj.1.0032>
- Tanaka, R., Makishima, A., & Nakamura, E. (2008). Hawaiian double volcanic chain triggered by an episodic involvement of recycled material: Constraints from temporal Sr–Nd–Hf–Pb isotopic trend of the Loa-type volcanoes. *Earth and Planetary Science Letters*, 265(3–4), 450–465. <https://doi.org/10.1016/j.epsl.2007.10.035>
- Taneja, R., O'Neill, C., Lackie, M., Rushmer, T., Schmidt, P., & Jourdan, F. (2015).  $^{40}\text{Ar}/^{39}\text{Ar}$  geochronology and the paleoposition of Christmas Island (Australia), Northeast Indian Ocean. *Gondwana Research*, 28, 391–406. <https://doi.org/10.1016/j.gr.2014.04.004>
- Wallace, P., Frey, F. A., Weis, D., & Coffin, M. F. (2002). Origin and evolution of the Kerguelen Plateau, Broken Ridge and Kerguelen Archipelago: Editorial. *Journal of Petrology*, 43, 1105–1108. 2002



- Weis, D., & Frey, F. A. (2002). Submarine Basalts of the Northern Kerguelen Plateau: Interaction Between the Kerguelen Plume and the Southeast Indian Ridge Revealed at ODP Site 1140. *Journal of Petrology*, 43, 1287–1309.
- Weis, D., Garcia, M. O., Rhodes, J. M., Jellinek, M., & Scoates, J. S. (2011). Role of the deep mantle in generating the compositional asymmetry of the Hawaiian mantle plume. *Nature Geoscience*, 4, 831–838.
- Weis, D., Kieffer, B., Maerschalk, C., Barling, J., de Jong, J., Williams, G. A., et al. (2006). High-precision isotopic characterization of USGS reference materials by TIMS and MC-ICPMS. *Geochemistry, Geophysics, Geosystems*, 7, Q08006. <https://doi.org/10.1029/2006GC001283>
- White, W. M. (1985). Sources of oceanic basalts: Radiogenic isotopic evidence. *Geology*, 13(2), 115–118. [https://doi.org/10.1130/0091-7613\(1985\)13<115:SOOBRI>2.0.CO;2](https://doi.org/10.1130/0091-7613(1985)13<115:SOOBRI>2.0.CO;2)
- White, W. M., Albarede, F., & Telouk, P. (2000). High-precision analysis of Pb isotope ratios by multi-collector ICP-MS. *Chemical Geology*, 167(3–4), 257–270. [https://doi.org/10.1016/S0009-2541\(99\)00182-5](https://doi.org/10.1016/S0009-2541(99)00182-5)
- White, W. M., & Duncan, R. A. (1996). In A. Basu & S. R. Hart (Eds.), *Geochemistry and geochronology of the Society Islands: New evidence for deep mantle recycling*, in *Earth processes: Reading the isotopic code*, *Geophysical Monograph Series* (Vol. 95, pp. 183–206). Washington, DC: American Geophysical Union.
- Woodhead, J. D. (1992). Temporal geochemical evolution in oceanic intra-plate volcanics: A case study from the Marquesas (French Polynesia) and comparison with other hotspots. *Contributions to Mineralogy and Petrology*, 111, 458–467. <https://doi.org/10.1007/BF00320901>
- Workman, R. K., Hart, S. R., Jackson, M. G., Regelous, M., Farley, K. A., Blusztajn, J., & Kurz, M. D. (2004). Recycled metasomatised lithosphere as the origin of the Enriched Mantle II (EM2) end-member: Evidence from the Samoan Volcanic Chain. *Geochemistry, Geophysics, Geosystems*, 5, Q04004. <https://doi.org/10.1029/2003GC000623>
- Wörner, G., Zindler, A., Staudigel, H., & Schmincke, H. U. (1986). Sr, Nd, and Pb isotope geochemistry of Tertiary and Quaternary alkaline volcanics from West Germany. *Earth and Planetary Science Letters*, 79, 107–119.
- Wright, E., & White, W. M. (1987). The origin of Samoa: New evidence from Sr, Nd, and Pb isotopes. *Earth and Planetary Science Letters*, 81, 151–162. [https://doi.org/10.1016/0012-821X\(87\)90152-X](https://doi.org/10.1016/0012-821X(87)90152-X)
- Yamamoto, J., Korenaga, J., Hirano, N., & Kagi, H. (2014). Melt-rich lithosphere-asthenosphere boundary inferred from petit-spot volcanoes. *Geology*, 42(11), 967–970. <https://doi.org/10.1130/G35944.1>
- Zindler, A., & Hart, S. (1986). Chemical geodynamics. *Annual Review of Earth and Planetary Sciences*, 14, 493–571.